



Real Time Finite Element Simulation of Thick and Thin Sandwich Plate with Viscoelastic Core and Embedded SMA Wires

Aidin Ghaznavi^{1,*}, Mohammad Shariyat²

¹ Renewable Energies Department, Niroo Research Institute (NRI), Tehran, Iran

² Faculty of Mechanical Engineering, K.N. Toosi University of Technology, Tehran, Iran

Abstract

In this paper, nonlinear dynamic analysis of sandwich plate with viscoelastic and flexible core and shape memory alloy embedded composite face sheets is performed. In order to simulate the dynamic behavior of sandwich plate, a higher order global-local theory based on the superposition principle is used. One of the most important advantage of presented theory is considering the thickness variation and transverse shear stresses, which is especially necessary in the study of thick sandwiches with soft core. In order to simulate the behavior of the shape memory alloy (SMA) wires, material properties variation are considered continuously in whole of the plate. In order to accurately investigate the behavior of the shape memory alloy, a written code is using an algorithm for solving the dynamic phase transformation base on modified Brinson model. The kinematic equations of phase transformation of embedded SMA wires are coupled with the equations of motion that leads to the nonlinearity and complexity of the equations. So to solve the equations, a development iterative method based on the formulation of nonlinear transient finite elements method with a dynamic phase transformation algorithm is used. The results show that the vibration amplitude of the sandwich plate is reduced due to energy dissipation because of the phase transformation of the SMA wires. Also, the core of the sandwich plate is considered of viscoelastic material. Due to the specific properties of the viscoelastic materials, the dynamic behavior of the structure and its consequence, the overall damping of the structure is affected. One of the previously unexplored studies is the simultaneous investigation of the damping effect of viscoelastic cores and embedded SMA wires. In other words, in this case, the sandwich plate has two different damping mechanisms with different function and nature that affect each other.

Keywords: Sandwich plate; Global-local theory; Dynamic behaviour; Flexible viscoelastic core; Shape Memory alloy; three-dimensional elasticity correction

1. Introduction

In the last decades, with the development of science and technology in the world, new and growing needs in

* Corresponding author. Tel.: 98-9397460060; fax: +98-2188364616.
E-mail address: aghaznavi@nri.ac.ir, aidin.ghaznavi@yahoo.com

different sciences and industries have led to the development of new materials and structures that can meet the needs of different fields. Among these materials, which are used in various industries due to their different properties, are composites made in combination with various materials such as shape memory alloys (SMA) and viscoelastic materials. Shape memory alloys are different from other metals because they are capable of performing the solid-to-solid phase transformation which is used for a variety of engineering purposes; Because of this ability, depending on the stress and temperature, this material has two different crystalline lattice structures. Therefore, shape memory alloys have two distinct capabilities: 1) Shape memory effect (SME), 2) Super Elastic Effect (SE) [1].

It should be mentioned that for viscoelastic materials, viscoelastic behaviour, unlike elastic behaviour, continuously depreciates mechanical energy during loading process. Whereas in fully elastic materials, mechanical energy is stored during loading process and released after loading. Some of the most important engineering materials when dealing with external forces simultaneously store and depreciate the applied mechanical energy. Such a structural reaction is called viscoelastic behaviour. The structural equations of viscoelastic behaviour inherently include not only stress and strain but also the rates of stress and strain changes. The behaviour of an elastic material is similar to that of a spring, while the behaviour of a viscoelastic material is measured with a damper [2]. So in general, a model can be designed to investigate the behaviour of a viscoelastic material with a combination of springs and dampers.

One of the first studies on composites with embedded SMA was conducted by Rogers in 1990 [3]. Ostachowicz et al. [4, 5] calculated natural frequency and buckling of composite plate with SMA using first shear order theory. Their results show that the use of SMA wires has a great effect on increasing the natural frequency of the structure and the critical buckling temperature. Turner [6] developed a fundamental model and finite element formulation to investigate the thermo mechanical response of composites with SMA under thermal and mechanical loads. Tsai and Chen [7] investigated the dynamic stability of composite beams reinforced with SMA wires under harmonic forces. Roh and Kim [8] investigated the optimization of composite sheets with SMA wires under low velocity impacts. Roh and Kim [9] also studied the low velocity impact of a composite sheet with SMA wires, except that they used one-dimensional constitutive model of shape memory alloys to simulate SMA wires, while in their previous research experimental values for simulation SMA behaviour.

It is also worth noting that extensive studies have been conducted on composite and viscoelastic plates. When the theory of viscoelastic was developed by researchers, the solution method was based on Laplace transforms. Laplace transform equations are used in stress-strain, strain-displacement relations [2]. Hashin [10] examined viscoelastic issues with constant properties. Wang and Tsai [11] used a finite element method to analyse the quasi-static and dynamic analysis of linear viscoelastic sheets. In studying the viscoelastic properties, Lake and Wineman [12] changed the Poisson's coefficient. They concluded that the Poisson's ratio in viscoelastic materials is time-dependent or has a complex frequency ratio. Yang et al. [13] examined the vibrational and damping effects of composite plates made of a combination of crane fibres and viscoelastic layers. Various studies have also been conducted to solve the elastic and orthotropic structure. Eshmatov [14] uses the Kelvin–Voigt model and provides an exponential function for its relaxation function. Actual models based on these assumptions cannot really show the effect of dynamic loading. If the same assumptions are made for nonlinear models, an integral differential equation is created, which in many cases can be solved by numerical methods such as Runge-Kutta. The numerical method developed by Eshmatov allows to solve systems that have nonlinear integral differential equations. Schovanec et al. [15] have studied fixed cracks, static and dynamic crack propagation in non-homogeneous viscoelastic materials under shear conditions. Schovanec and Walton [16] examined the conditions of crack propagation in a heterogeneous linear viscoelastic object under quasi-static loading and calculated the released energy ratio. Assie et al. [17] obtained the dynamic response of impact on a viscoelastic plate by a finite element. The methods used were such that the equation of motion was obtained integrally. A solid linear viscoelastic model was used to describe the viscoelastic behaviour. Also Assie et al. [18] investigated the behaviour of viscoelastic composite plates under triangular loading; they used the Richard model to describe the viscoelastic properties. Zhang et al. [19] studied the free vibration and damping analysis of porous functionally graded sandwich plates with a viscoelastic core based on a modified Fourier-Ritz method. In their study, Sandwich plate made of a viscoelastic core and porous FG face sheets. Hosseini and Khorasani [20] presented a finite element formulation for dynamic analysis of sandwich plates with viscoelastic core under large deformation using incremental updated Lagrangian approach together with the Newmark integration scheme. Sheng et al. [21] examined analytically and experimentally vibration characteristics of a sandwich plate with viscoelastic core. They found that sandwich with periodic constrained-layer damping treatment had better performance comparing to the traditional constrained-layer damping behaviour. Ledi et al. [22] presented a new method for the studying the viscoelastic material properties of a symmetric three layered viscoelastic sandwich beam. Also their using the experimental vibration tests to determine resonant frequencies and loss factors.

Sandwich plates are one of the most important structures in which SMA wires or viscoelastic materials are used. Since the three-dimensional analytical solution of sandwich plates has many limitations, the analysis of such

structures based on the two-dimensional theory of plates and shells is very practical and noteworthy. The basis of these theories is to convert three-dimensional models to two-dimensional by eliminating the dependence of the model on thickness. For this purpose, various methods such as equivalent single-layer theories, layer wise theories, and theories based on the principle of superposition (zigzag and global-local) have been proposed [23]. However, some of the theories presented also have shortcomings. For example, if there are significant changes between the properties of the layers or if the structure is made up of a large number of layers, global theories will not be able to properly assess local displacements. As a result, calculated strain and stress by these theories will not be accurate. Thus, equivalent single-layer theories such as classical theory (CLT), first-order shear theory (FSDT), and upper-order shear theory (HSDT) [24-27] do not provide accurate results in such cases. Equivalent single-layer theories [28-31] are commonly used to analyse the overall behaviour of structures. In layer wise theories, each layer of the plate or shell is considered as an independent layer, and in each layer, the description of the displacement field is used independently. The resulting models are also called layered (local) or local theories [32-35]. Although this theory has good accuracy and correctly displays the zigzag effects of displacement in composites, the number of independent parameters depends on the number of layers and therefore the time of their calculations is high [36]. Therefore, theories based on the principle of superposition were presented that in addition to considering the global and local behaviour of the sandwich plate, it has fewer independent parameters and independent of the number of layers and therefore requires less time to analyse the structure [37]. Totally, a limited number of papers have been published for studying the dynamic and static response of the sandwich plates with flexible soft core. These include published articles by Moreira and Rodrigues [38], Elmalich and Rabinovitch [39], Rabinovitch and Frostig [40], Cetkovic and Vuksanovic [41], and Wu and Chen [42]. Also, Ghaznavi and Shariyat [43] presented a new higher order global-local theory for examining the static, frequency, and dynamic behaviour of sandwich plates with soft cores and auxetic core. Also they studied the behaviour of sandwich plates with flexible soft and hard cores and composite face sheets embedded SMA wires [44, 45]. They considered the behaviour of shape memory alloy to be symmetrical and asymmetrical which had a significant effect on the damping of sandwich plates [46]. Also the study of the behaviour of smart sandwiches has attracted the attention of many researchers in recent years [47-79].

In this paper, by presenting the higher global-local theory based on the superposition principle, which can consider changing the thickness of the core accurately, the behaviour of thick and thin sandwich plates with embedded SMA wires in the composite face sheets as well as viscoelastic core is analysed. One of the most important features of the presented theory is the correction of obtained shear stresses and the effect of this correction on the total results. It should be mentioned that kinematic equations of SMA phase transformation are coupling with motion equations, which leads to the nonlinearity and complexity of problem. For this purpose, an incremental iterative method based on the nonlinear transient finite element formulation that merged with the mentioned dynamic phase transformation algorithm has been used to solve the equations. Initially, the performance of the modified Brinson model for simulating shape memory alloy behaviour under different conditions and various cyclic loads is investigated. In the following, the results of the dynamic analysis of thin and thick sandwich plates with composite face sheets with embedded SMA wires and flexible core or viscoelastic core are discussed and also the effect of different parameters of viscoelastic core on the overall behaviour of the sandwich and its damping is investigated. Finally, the results of the different cases are compared with each other. It should be mentioned that in order to increase the accuracy of the model, the behaviour of SMA wires is considered asymmetric in tension and pressure, which is a more realistic assumption, therefore a more accurate estimate of the role of embedded SMA wires in structural damping is obtained.

2. The Governing Equations of Phase Transformation and Motion of Sandwich Plate with Viscoelastic Core and SMA Wires Embedded in Composite Face Sheets

2.1. Description of The Displacement Field According to The Presented Theory

The geometry of the studied sandwich plate and coordinate system and the considered deformation kinematics are presented in Figure 1. The origin of the general coordinate system is located on the middle page of the sandwich and the z axis is considered positive upwards. The length and width of the sandwich sheet in the direction of x and y are denoted a and b , respectively, the total thickness of the sandwich plate is denoted H . Also, the thickness of the upper layer, the thickness of the core and the thickness of the lower layer are considered h_1 , h_2 , h_3 respectively.

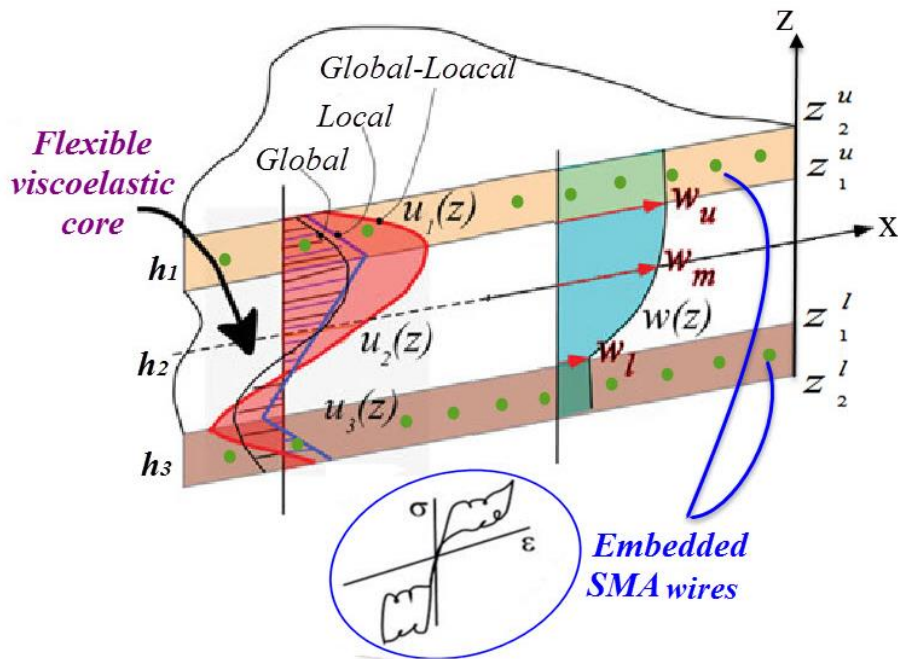


Fig 1: Geometrical parameters and deformation kinematics of the in-plane and out of plane displacement components of the considered sandwich plate with composite face sheets embedded SMA wires and a flexible viscoelastic core.

Regarding SMA wires, it should be noted that the SMA wires are placed on both the upper and lower surface in both x and y directions (perpendicular to each other) and also is considered that the wires are placed in the middle of each face sheet. In the following, deformation field of the three-layer sandwich plate is presented. Generally, the in-plane displacement components are considered to be composed of global as well as local terms:

$$\begin{cases} u(x, y, z, t) = \\ u_G(x, y, z, t) + u_L^k(x, y, z, t) \\ v(x, y, z, t) = \\ v_G(x, y, z, t) + v_L^k(x, y, z, t) \end{cases} \quad (1)$$

$$(k = 1, 2, 3)$$

Where u_G and v_G are the global and u_L and v_L are the local components. After imposing the continuity conditions of the displacement components at the interfaces between layers and by using third-order global and first order local components, Eq. (1) eventually leads to the following:

$$\begin{aligned} U = & \mathcal{H} \left[z - z_1^u \right] \left\{ u_0 + z \varphi_x(x, y, t) + z^3 \lambda_x(x, y, t) + (z - z_1^u) \varphi_x^{(1)}(x, y, t) + z_1^u \varphi_x^{(2)}(x, y, t) \right\} \\ & + \mathcal{H} \left[z(z_1^l + z_1^u) - z^2 - z_1^l z_1^u \right] \left\{ u_0 + z [\varphi_x(x, y, t) + \varphi_x^{(2)}(x, y, t)] + z^3 \lambda_x(x, y, t) \right\} \end{aligned} \quad (2)$$

$$\begin{aligned} V = & \mathcal{H} \left[z - z_1^u \right] \left\{ v_0 + z \varphi_y(x, y, t) + z^3 \lambda_y(x, y, t) + (z - z_1^u) \varphi_y^{(1)}(x, y, t) + z_1^u \varphi_y^{(2)}(x, y, t) \right\} \\ & + \mathcal{H} \left[z(z_1^l + z_1^u) - z^2 - z_1^l z_1^u \right] \left\{ v_0 + z [\varphi_y(x, y, t) + \varphi_y^{(2)}(x, y, t)] + z^3 \lambda_y(x, y, t) \right\} \end{aligned} \quad (3)$$

$$+ \mathcal{H} \left[z_1^l - z \right] \left\{ v_0 + z \varphi_y(x, y, t) + z^3 \lambda_y(x, y, t) + (z - z_1^l) \varphi_y^{(3)}(x, y, t) + z_1^l \varphi_y^{(2)}(x, y, t) \right\}$$

Where \mathcal{H} is the Heaviside's function. As shown in Eq. (2) and Eq. (3), the final deformation of the sheet is calculated based on the principle of superposition. The purpose of this superposition is to simultaneously consider

the effect of the displacement field of each layer along with the effect of the total displacement of the sandwich sheet so that the behavior of each layer can be studied separately and accurately, While not ignoring the overall behavior of the sandwich sheet and consider its effect on the behavior of each layer. In other words, the major defect of layer wise theories that neglect the general behavior of the sandwich panel is covered by using this method. And also, the defect of equivalent single-layer theories such as third shear order theory, etc., which ignores the behavior of each layer separately and only studies the behavior of the whole plate, has also been well resolved. Note that, based on the present description of deformation kinematics, the net rotations of the layers are now non identical and variable. As it was mentioned, one of the advantages of the presented theory is to consider the changes of transvers displacement of the sandwich panel (W) as follow:

$$w = \mathcal{H} \left[z - z_1^u \right] w_u + \mathcal{H} \left[z_1^l - z \right] w_l + \mathcal{H} \left[z (z_1^l + z_1^u) - z^2 - z_1^l z_1^u \right] \left\{ \mathcal{L}_1(z) w_u + \mathcal{L}_2(z) w_m + \mathcal{L}_3(z) w_l \right\} \tag{4}$$

Where \mathbf{H} is the Heaviside's function and w_u, w_l, w_m are denoted out of plane deflection of the upper and lower composite face sheet and the middle plane of the core respectively, and $\mathcal{L}_i(z)$ are interpolation functions.

As can be seen in Eq. (4), since rigidity of the upper and bottom layer of sandwich face sheets is much higher and their thickness is much smaller than those of the core, a uniform and a quadratic transverse distribution of the out of plane deflection w are adopted for the face sheets and the core, respectively. Therefore, a three-layer sandwich plate has a total of 15 independent displacement parameters:

$$u_0, v_0, \varphi_x, \varphi_y, \lambda_x, \lambda_y, \varphi_x^{(1)}, \varphi_y^{(1)}, \varphi_x^{(2)}, \varphi_y^{(2)}, \varphi_x^{(3)}, \varphi_y^{(3)}, w_u, w_m, w_l$$

2.2. The Finite Element Form of the Motion Governing Equations of Sandwich Panel

It should be noted that all theories of plate and shell, including global-local theory, are two-dimensional, so a two-dimensional finite element method must be used to solve them. In this regard, a representative plane, e.g., the mid surface of the plate, may be discretized by means of appropriate elements and shape function. In the present research, nine-node quadrilateral elements are used to trace in-plane variations of the displacement components:

$$\Phi(x, y, t) = \mathcal{N}(x, y) \Phi^{(e)}(t) \tag{5}$$

In which, \mathcal{N} and $\Phi^{(e)}$ respectively, are denoted the shape functions matrix and vector of the nodal values of the displacement. According to Eq. (5):

$$\psi(x, y, z, t) = \mathbf{H}(z) \mathcal{N}(x, y) \Phi^e(t) = \Gamma(x, y, z) \Phi^e(t) \tag{6}$$

The stress components may be computed according to the generalized Hooke's law as follows:

$$\sigma = \begin{Bmatrix} \sigma^{(1)} \\ \sigma^{(2)} \\ \sigma^{(3)} \end{Bmatrix} = \begin{bmatrix} C^{(1)} & 0 & 0 \\ 0 & C^{(2)} & 0 \\ 0 & 0 & C^{(3)} \end{bmatrix} \begin{Bmatrix} \varepsilon^{(1)} \\ \varepsilon^{(2)} \\ \varepsilon^{(3)} \end{Bmatrix} = \hat{Q} \varepsilon = \hat{Q} \Lambda(x, y, z) \Phi^{(e)}(t) \tag{7}$$

Where $C(i)$, ($i = 1, 2, 3$) is the matrix of the elastic parameters in the transformed, i.e., geometric, coordinates of the sandwich plate. The governing equations are calculated through using Hamilton's principle. If the strain energy and work of the externally applied loads (including the inertia forces) are denoted by U and V , respectively, one may write as follows [24]:

$$\delta U - \delta W = 0 \tag{8}$$

$$\delta U = \int_{\Omega} (\delta \varepsilon)^T \sigma d\Omega = \int_{\Omega} (\delta \Phi^{(e)})^T \Lambda^T \hat{Q} \Lambda \Phi^{(e)} d\Omega \tag{9}$$

$$\delta W = \int_A q \delta w_u dA - \int_{\Omega} \rho (\delta \Phi^{(e)})^T \ddot{\Phi} d\Omega \tag{10}$$

Where A, Ω, q are area and volume of the element, intensity of the externally applied distributed load to the sandwich plate, respectively. Substituting Eq. (9) and Eq. (10) into Eq. (8) leads to the following result, for any arbitrary time interval:

$$(\delta \Phi^{(e)})^T \left[\int_{\Omega} \rho \Gamma^T \Gamma \ddot{\Phi} d\Omega + \int_{\Omega} \Lambda^T \hat{Q} \Lambda \Phi^{(e)} d\Omega - \int_A q (R \mathcal{N})^T dA \right] = 0 \tag{11}$$

Since $\delta \Phi^{(e)}$ is an arbitrary and generally nonzero vector, the governing equation of the sandwich plate becomes:

$$[\int_{\Omega} \rho \Gamma^T \Gamma d\Omega] \ddot{\Phi}^{(e)} + [\int_{\Omega} \Lambda^T \hat{Q} \Lambda d\Omega] \Phi^{(e)} = \int_A q (R \mathcal{N})^T dA \tag{12}$$

or in a compact form

$$M \ddot{\Phi}^{(e)} + K \Phi^{(e)} = F \tag{13}$$

Which various algorithms can be used to solve Eq. (13); the algorithm used in this paper is Newmark’s method, which has a higher accuracy for dynamic problems.

2.3. Modified the Motion Governing Equations of Sandwich Panel with Embedded Shape Memory Alloy Wires in Composite Face Sheets

In this section, the obtained governing equations are modified base on considering the embedded SMA wires in the composite face sheets of sandwich panel. In the initial conditions, SMA wires are without any tension, but since the sandwich plate is subjected to mechanical loads, the supralastic behavior due to phase transformation of the SMA wires appears in the stress-strain relations of the corresponding layer. In other words the SMA wire shows a pseudo-elastic behavior at temperatures higher than the austenite finish temperatures (A_f). Loading the SMA lower than the martensite start stress (σ_{Ms}) leads to the martensite to austenite phase transformation and unloading to stress levels below the austenite start (σ_{As}) activates a martensite to austenite phase transformation. These phase transformation makes a hysteresis loop in the strain-stress curve of the SMA wires. The resulting hysteresis loop may consume a remarkable portion of the surrounding energies. The modified pseudo-elastic Brinson’s constitutive law of the SMA may be rewritten as [45]:

$$\begin{aligned} \sigma &= \sigma_0 + [(\varepsilon - \varepsilon_0) + (\xi_0 - \xi_s) \varepsilon_L] E_A + [\xi_s - \xi_0 \varepsilon_0 + (\xi_0 \xi_{s0} - \xi \xi_s) \varepsilon_L] (E_M - E_A) \\ \xi &= \xi_s + \xi_T \end{aligned} \tag{14}$$

Where E_A , E_M , ε_l are denoted moduli of the martensite and austenite phases of the SMA, the maximum recoverable strain, respectively, and the subscript “0” associates with global or local events of phase transformations and are time-history-dependent and non-stationary values as they change at the beginning of each event. ξ_T represents the fraction of the material that is purely temperature-induced martensite with multiple variants and ξ_s denotes the fraction of the material that has been transformed, or oriented, by stress into a single martensite (detwined) variant, and ξ shows total martensite volume fraction. The transformation calculations may be divided into the different regions [46].

It should be noted that theses parameters are different in tension and compression. ξ_{s0} is initial martensite volume fraction and ξ_s is the stress-induced martensite volume fraction before the current transformation. Because of the embedded SMA wires and their pseudoelasticity effect, the stress-strain relation of the layer with SMA wires is modified as follows:

$$\sigma = \begin{bmatrix} \sigma_1 \\ \sigma_2 \\ \sigma_3 \\ \sigma_4 \\ \sigma_5 \\ \sigma_6 \end{bmatrix} = \begin{bmatrix} C_{11}^* & C_{12}^* & C_{13}^* & 0 & 0 & 0 \\ C_{12}^* & C_{22}^* & C_{23}^* & 0 & 0 & 0 \\ C_{13}^* & C_{23}^* & C_{33}^* & 0 & 0 & 0 \\ 0 & 0 & 0 & C_{44}^* & 0 & 0 \\ 0 & 0 & 0 & 0 & C_{55}^* & 0 \\ 0 & 0 & 0 & 0 & 0 & C_{66}^* \end{bmatrix} \begin{bmatrix} \varepsilon_1 \\ \varepsilon_2 \\ \varepsilon_3 \\ \varepsilon_4 \\ \varepsilon_5 \\ \varepsilon_6 \end{bmatrix} - \begin{bmatrix} V_{sx} \{ \sigma_0 + [(\xi_{s0} - \xi) \varepsilon_L - \varepsilon_0] E_A + \\ [(\xi_0 \xi_{s0} - \xi \xi_s) \varepsilon_L - \xi_0 \varepsilon_0] (E_M - E_A) \} \\ V_{sy} \{ \sigma_0 + [(\xi_{s0} - \xi) \varepsilon_L - \varepsilon_0] E_A + \\ [(\xi_0 \xi_{s0} - \xi \xi_s) \varepsilon_L - \xi_0 \varepsilon_0] (E_M - E_A) \} \\ 0 \\ 0 \\ 0 \\ 0 \end{bmatrix} \tag{15}$$

Where V_{sx} , V_{sy} are the volume fraction and the modulus of elasticity of the embedded SMA wires in the intended composite layer in x and y directions, respectively. As it was mentioned before, Stress-strain diagram of the SMA is usually an asymmetric one which the tensional transformation stresses are smaller and the relevant strains are larger [81-85]. In present research, anisotropy of the SMA behaviors is considered the dynamic analysis of sandwich plates with embedded SMA wires; so Eqs. (15) can be rewrite as follow:

$$\sigma = \begin{cases} \mathcal{C}_t^*(\zeta)\varepsilon - \sigma_t^S; \\ \text{SMA wires in tension} \\ \mathcal{C}_c^*(\zeta)\varepsilon - \sigma_c^S; \\ \text{SMA wires in compression} \end{cases} \tag{16}$$

Where the *t* and *c* subscripts denote for the tensile and compressive stresses, respectively. There is no obligation to alignment of the SMA wires with the main directions of the composite plate, so the wires can be angled with the main directions of the composite plate. In the geometric coordinates system of the composite plate, which θ is the angle of the SMA wires with the x-axis of the intended plate, we can express Eq. (16) with the use of rotational transformation matrix as follows:

$$\sigma = \mathcal{TC}^*(\zeta)\varepsilon - \hat{\sigma}^s = \hat{Q}(\zeta)\varepsilon - \hat{\sigma}^s \tag{17}$$

Where \mathcal{T} is the rotational transformation matrix and $\hat{\sigma}^s$ is as follow:

$$\hat{\sigma}^s = \begin{cases} V_{sx} \operatorname{sgn}(\sigma) E_{sx} \xi_s \varepsilon_L \cos^2 \theta + V_{sy} \operatorname{sgn}(\sigma) E_{sy} \xi_s \varepsilon_L \sin^2 \theta \\ V_{sx} \operatorname{sgn}(\sigma) E_{sx} \xi_s \varepsilon_L \sin^2 \theta + V_{sy} \operatorname{sgn}(\sigma) E_{sy} \xi_s \varepsilon_L \cos^2 \theta \\ 0 \\ 0 \\ 0 \\ V_{sx} \operatorname{sgn}(\sigma) E_{sx} \xi_s \varepsilon_L \sin \theta \cos \theta - V_{sy} \operatorname{sgn}(\sigma) E_{sy} \xi_s \varepsilon_L \sin \theta \cos \theta \end{cases} \tag{18}$$

Where E_{sx} and E_{sy} are the modulus of elasticity of the SMA wires in the x and y directions, respectively. These moduli are related to the volume fraction of the SMA according to Voigt (rule of mixtures) model that can be different in x and y directions:

$$E(\xi) = E_A + \xi(E_M - E_A) \tag{19}$$

For a composite layer containing SMA wires, the equivalent material properties of the composite layer, in the wire axes directions, may be computed as follow:

$$\begin{cases} E_l(\xi_s) = E_l^c(1 - V_s) + E_s(\xi_s) V_s \\ E_t(\xi_s) = E_t^c / \{1 - \sqrt{V_s} [1 - E_t^c / E_s(\xi_s)]\} \\ G_{lt}(\xi_s) = G_{lt}^c G_s(\xi_s) / [(1 - V_s) G_s(\xi_s) + V_s G_{lt}^c] \\ \nu_{lt} = \nu_{lt}^c(1 - V_s) + V_s \nu_s \\ \rho = V_c \rho_c + V_s \rho_s \end{cases} \tag{20}$$

Where subscripts *s*, *c*, *l* and *t* denote SMA, composite and directions parallel and normal to the SMA wire, respectively. In addition to the effect of SMA wires phase transformation, which makes the equations nonlinear, the effect of force due to the presence of SMA wires should also appear in governing equations and finite element relations of sandwich panel. By considering this effect, the principle of minimum total potential energy is rewritten as follows:

$$\delta U = \int_{\Omega} (\delta \varepsilon)^T \sigma d\Omega = \int_{\Omega} (\delta \Phi^{(e)})^T \Lambda^T (\mathcal{TC}^* \Lambda \Phi^{(e)} - \hat{\sigma}^s) d\Omega \tag{21}$$

$$\begin{aligned} \delta W &= \int_A q \delta w_u dA - \int_{\Omega} \rho (\delta \Phi^{(e)})^T \ddot{\Phi} d\Omega \\ &= \int_A q (\delta \Phi^{(e)})^T (R \mathcal{N})^T dA - \int_{\Omega} \rho (\delta \Phi^{(e)})^T \mathcal{N}^T \mathcal{N} \ddot{\Phi}^{(e)} d\Omega \end{aligned} \tag{22}$$

By replacing the above equations in the minimum total potential energy principle:

$$(\delta \Phi^{(e)})^T \left[\int_{\Omega} \rho \mathcal{N}^T \mathcal{N} \ddot{\Phi}^{(e)} d\Omega + \int_{\Omega} \Lambda^T \mathcal{TC}^* \Lambda \Phi^{(e)} d\Omega - \int_{\Omega} \Lambda^T \hat{\sigma}^s d\Omega - \int_A q (R \mathcal{N})^T dA \right] = 0 \tag{23}$$

Finally:

$$M\ddot{\Psi} + [K(\Psi)]\Psi = [F(\Psi)] \tag{24}$$

Where in the above equation, $K(\Psi)$ and $F(\Psi)$ matrices are related to the SMA wires status. In other words, the effect of SMA wires appears in two forms in equations. Depending on the state of the material in terms of the level of stress and the applied load, the phase of the shape memory alloy is determined, and as a result, the physical properties of the SMA wires, including their Young's modulus, are determined and effectively are affected $K(\Psi)$ in the Eq. (24). But σ^s substantially has a force nature. Therefore, it can be summed up with the force vector (right component of Equation (24)). In other words, the force vector is also affected by the SMA wires. Therefore, in Eq. (24), the stiffness matrices and the force vector are a function of the martensitic volume fractional (ξ) of SMA wires. On the other hand, martensitic volume fractional (ξ) changes momentary in different parts of the composite face sheets, and at different times. Since martensitic volume fraction is a function of stress distribution and it is also a function of the displacement field, therefore, the martensitic volume fractional (ξ) and totally the properties of the material are unknown parameters. As a result, the presence of SMA wires in the sandwich panel leads to complexity and non-linearity of governing equations. Therefore, in order to solve these nonlinear dynamic equations, an iterative method has been proposed, which is presented in detail at the following sections.

2.4. Modeling Viscoelastic Behavior of the Sandwich Core Using Real Time Finite Element Simulation

In viscoelastic materials, the material's response is affected by its loading rate, followed by a slow and continuous change in the response at a decreasing rate. The rate of loading affects the time dependent response of a viscoelastic material. For instance, the longer it takes to reach the final value of stress at a constant rate of loading, the larger the corresponding strain. For this reason, viscoelastic materials store a history of their response and have some kind of memory. This memory effect is evident in the constitutive relationship between the stress and strain tensors [86]. One way to determine these constitutive equations for linear viscoelastic materials is to use the Boltzmann superposition principle. Suppose an arbitrary strain input is coming through superposition of small strain increments:

$$\varepsilon(t) = \sum_{j=1}^n \Delta\varepsilon_j = \int_0^t d[\varepsilon(s)] \tag{25}$$

Where “s” is any arbitrary time interval between time 0 and t that the strain is assumed to be constant during it. The increase in strain up to time “t” is related to the corresponding stress increments by using following Hooke's law:

$$\sigma(t) = \sum_{j=1}^n \Delta\sigma_j(t - s_j) = \sum_{j=1}^n E(t - s_j)\Delta\varepsilon_j \tag{26}$$

By considering the appropriate ranges, the following constitutive equation can be supposed:

$$\sigma(t) = \int_0^t E(t - s) \frac{\partial\varepsilon(s)}{\partial s} ds \tag{27}$$

The generalized Maxwell solid model is typically used to simulate viscoelastic solid materials [87-88] that is a combination of springs and dashpots. This model can be written in the form of prony series for the stress relaxation function as follows:

$$E(t) = E_\infty + \sum_{j=1}^N E_j e^{\left(\frac{-t}{\tau_j}\right)} \tag{28}$$

Where N is the number of Maxwell elements, E_j is the elastic coefficient (E_∞ is the long-term elastic modulus corresponding to the system's steady-state elastic response), and τ_j is the relaxation time related to the damping coefficients of dashpots as $\frac{\eta}{E_\infty}$. By replacing the above equation in Eq. (28) and separating its viscoelastic and elastic terms from each other, it can be written:

$$\sigma(t) = \int_0^t E_\infty \frac{\partial\varepsilon(s)}{\partial s} ds + \int_0^t \sum_{j=1}^N E_j e^{\left(\frac{-t}{\tau_j}\right)} \frac{\partial\varepsilon(s)}{\partial s} ds = E_\infty \varepsilon(t) + \sum_{j=1}^N \int_0^t E_j e^{\left(\frac{t-s}{\tau_j}\right)} \frac{\partial\varepsilon(s)}{\partial s} ds = \sigma_0(t) + \sum_{j=1}^N \mathcal{R}_j(t) \tag{29}$$

By defining a time step $\Delta t = t_{n+1} - t_n$, that t_{n+1} and t_n indicate the time of the current step and the time of the previous step, respectively, and also by considering $\varepsilon(t) = \frac{\sigma(t)}{E_\infty}$, it is possible to present recursive formula for internal stress variables. The transition from differential coefficient to discrete time steps leads [80]:

$$\mathcal{X}_j^{n+1} = e^{\left(\frac{-\Delta t}{\tau_j}\right)} \mathcal{X}_j^n + \gamma_j \int_{t_n}^{t_{n+1}} e^{\left(\frac{-t_{n+1}-s}{\tau_j}\right)} ds \frac{\sigma_0^{n+1} - \sigma_0^n}{\Delta t} \tag{30}$$

Where $\gamma_j = E_j / E_\infty$ is the normalized elastic modulus of the j^{th} element. Eq. (40) can rewrite in a recursive formula in 3D tensor representation by integrating analytically [80]:

$$\mathcal{X}_j^{n+1} = e^{\left(\frac{-\Delta t}{\tau_j}\right)} \mathcal{X}_j^n + \gamma_j \frac{1 - e^{\left(\frac{-\Delta t}{\tau_j}\right)}}{\frac{\Delta t}{\tau_j}} (\sigma_0^{n+1} - \sigma_0^n) \tag{31}$$

Considering the internal stress variables defined by Eq. (32) and the elastic contribution, the stress of linear viscoelastic Maxwell material can be defined as follows:

$$\sigma^{n+1} = \sigma_0^{n+1} + \sum_{j=1}^N \mathcal{X}_j^{n+1} \tag{33}$$

To obtain governing equations in the finite element form, the same path of linear elastic materials is applied. As was mentioned in previous sections, the FE form of the elastic material is:

$$\begin{aligned} \sigma_0^{n+1} &= \hat{Q}(\zeta) \varepsilon^{n+1} - \hat{\sigma}^s(\sigma_0, \varepsilon_0, \xi_{s0}, \xi) \\ \varepsilon &= \mathcal{D}\delta = \hat{Q}(\zeta) \Lambda(x, y, z) \Phi \end{aligned} \tag{34}$$

Where \hat{Q} is the elastic modulus matrix of the sandwich plate with embedded SMA wires in composite face sheets. So, based on the viscoelastic Maxwell material definition, the above equations can be modified as follow:

$$\begin{aligned} \sigma^{n+1} &= \hat{Q}_{infinity} \mathcal{D}\Phi^{n+1} + \sum_{j=1}^N \left[e^{\left(\frac{-\Delta t}{\tau_j}\right)} \mathcal{X}_j^n + \gamma_j A_j (\hat{Q}_{infinity} \mathcal{D}\Phi^{n+1} - \hat{Q}_{infinity} \mathcal{D}\Phi^n) \right. \\ &\quad \left. - \hat{\sigma}^s(\sigma_0, \varepsilon_0, \xi_{s0}, \xi) \right] \\ &= \hat{Q}_{infinity} \mathcal{D} \left(1 + \sum_{j=1}^N \gamma_j A_j \right) \Phi^{n+1} + \sum_{j=1}^N e^{\left(\frac{-\Delta t}{\tau_j}\right)} \mathcal{X}_j^n - \hat{Q}_{infinity} \mathcal{D} \left(\sum_{j=1}^N \gamma_j A_j \right) \Phi^n \\ &\quad - \hat{\sigma}^s(\sigma_0, \varepsilon_0, \xi_{s0}, \xi) \end{aligned} \tag{35}$$

Where $\hat{Q}_{infinity}$ is the stable modulus matrix of the viscoelastic material; and A_j is defined as follow:

$$A_j = \frac{1 - e^{\left(\frac{-\Delta t}{\tau_j}\right)}}{\frac{\Delta t}{\tau_j}} \tag{36}$$

Using the definition of internal force:

$$f_{int} = \int_{\Omega} [\Lambda^T \hat{Q} \Lambda d\Omega] \Phi = K \Phi \tag{37}$$

And considering Eq. (44), it can modified for the viscoelastic Maxwell material:

$$f_{int} = K_T \Phi^{n+1} + \mathcal{X}_{hist}^{n+1} - K_{hist} \Phi^n \tag{38}$$

Where Φ^{n+1} and Φ^n are the displacement vectors of nodes in the current time step and the previous time step. Also, K_T (tangent stiffness matrix) and K_{hist} (history stiffness matrix) include:

$$K_T = \mathcal{D}^T \hat{Q}_{infinity} \mathcal{D}V \left(1 + \sum_{j=1}^N \gamma_j A_j \right) \tag{39}$$

$$K_{hist} = \mathcal{D}^T \hat{Q}_{infinity} \mathcal{D}V \sum_{j=1}^N \gamma_j A_j \tag{40}$$

And \mathcal{H}_{hist}^{n+1} is the history vector at the current time step:

$$\mathcal{H}_{hist}^{n+1} = V \mathcal{D}^T \sum_{j=1}^N e^{\left(\frac{\Delta t}{\tau_j} \right)} \mathcal{H}_j^n \tag{41}$$

It is possible to rewrite \mathcal{H}_j^{n+1} for each element as follow:

$$\mathcal{H}_j^{n+1} = e^{\left(\frac{\Delta t}{\tau_j} \right)} \mathcal{H}_j^n + \gamma_j A_j \hat{Q}_{infinity} \mathcal{D} \left(\Phi^{n+1} - \Phi^n \right) \tag{42}$$

Finally, the constructive equation for sandwich panel with viscoelastic core and composite face sheets with embedded SMA wires can be rewritten in the following form:

$$M \ddot{\Psi}^{n+1} + [K_T(\Psi)] \Psi^{n+1} = [F(\Psi)] \tag{43}$$

$$F(\Psi) = [F_{ext}(\Psi) - F_{hist}]$$

Where F_{hist} is:

$$F_{hist} = \mathcal{H}_{hist}^{n+1} - K_{hist} \Phi^n \tag{44}$$

It should be mentioned that $K_T(\Psi)$ and $F_{ext}(\Psi)$ affected by the embedded SMA wires in the composite face sheets as explained in the previous section. In order to calculate the natural frequencies of sandwich plate, complex eigenvalue form of Eq. (44) is used. In order to calculate the natural frequencies of sandwich plate, the complex eigenvalue problem of Eq. (44) takes the form as Daya and Potier-Ferry can be written as follow [81]:

$$([K] - \omega^* [M]) \{\Phi\} = 0 \tag{45}$$

Where ω^* is the complex Eigen frequency. If the complex Eigen frequencies are obtained, the natural frequencies and the loss factors of the sandwich plate with the viscoelastic core and embedded SMA wires can be computed as follows [82]:

$$\omega = \sqrt{\text{Re} \left[\left(\omega^* \right)^2 \right]}, \quad \eta = \frac{\text{Im} \left[\left(\omega^* \right)^2 \right]}{\text{Re} \left[\left(\omega^* \right)^2 \right]} \tag{46}$$

2.5. Correction of the Results According to the Dynamic 3D Theory of Elasticity

Determining the transverse components of stress, especially the transverse shear stress components, is of great importance in the design process of sandwich structures. In most existing equivalent single-layer, layerwise, and even zigzag theories, transverse shear stresses are calculated with the approach of using governing equations directly. For this reason, the amount of shear stresses calculated between the layers is not continuous. This issue affects the accuracy of calculated shear stresses. For this reason, in many cases, such as first- shear order theory, it is necessary to use the shear correction factor [83]. Cho and Kim [84], Zhen and Chen [85] and Shariyat [86] have done a lot of research on sandwich plates with stiff cores and showed that even the third order shear deformation plate theory may lead a discrepancy of the order of 40% with respect to the 3D elasticity theory when a constitutive-law-

based formulation is applied. It is clear that for sandwich plates with soft cores, constitutive-law-based results are more unreliable. Although the presented global-local theory can accurately describe transverse variations of a sandwich plate with a flexible core, predictions of the whole displacement and stress fields of sandwich plate have to be modified based on the 3D theory of elasticity:

$$\sigma_{x,x} + \tau_{xy,y} + \tau_{xz,z} = \rho \ddot{u} \tag{47}$$

$$\sigma_{y,y} + \tau_{xy,y} + \tau_{yz,z} = \rho \ddot{v}$$

Therefore, it follows from Eq. (48) and Eq. (49):

$$\begin{aligned} \tau_{xz}^{(1)} &= \int_z^{z_1^u} \{ \rho \ddot{u}^{(1)} - (\sigma_{x,x}^{(1)} + \tau_{xy,y}^{(1)}) \} dz; & z_1^u \leq z \leq z_2^u \\ \tau_{xz}^{(2)} &= \int_z^{h_2/2} \{ \rho \ddot{u}^{(2)} - (\sigma_{x,x}^{(2)} + \tau_{xy,y}^{(2)}) \} dz + \tau_{xz}^{(1)} \Big|_{z=h_2/2}; & z_1^l \leq z \leq z_1^u \\ \tau_{xz}^{(3)} &= \int_z^{z_2^l} \{ \rho \ddot{u}^{(3)} - (\sigma_{x,x}^{(3)} + \tau_{xy,y}^{(3)}) \} dz \\ &= \int_z^{-h_2/2} \{ \rho \ddot{u}^{(3)} - (\sigma_{x,x}^{(3)} + \tau_{xy,y}^{(3)}) \} dz + \tau_{xz}^{(2)} \Big|_{z=-h_2/2}; & z_2^l \leq z \leq z_1^l \end{aligned} \tag{48}$$

And $\tau_{yz}^{(i)}$ is calculated in the same way. Then, after calculating the modified shear transverses stresses base on the 3D elasticity theory, the obtained results are applied for all whole calculation of the sandwich plate. For this purpose, modified transverse shear stresses for all nodes are replaced in the total stress matrix of the sandwich. Also using the following equations, the corrected displacement vector of the sandwich panel is obtained based on the corrected stress field:

$$\begin{aligned} \sigma^{n+1} \Big|_{corrected} &= \hat{Q}_{infinity} \mathcal{D} \left(1 + \sum_{j=1}^N \gamma_j A_j \right) \Phi^{n+1} + \sum_{j=1}^N e^{\left(-\frac{\Delta t}{\tau_j} \right)} \mathcal{X}_j^n \Big|_{corrected} \\ &- \hat{Q}_{infinity} \mathcal{D} \left(\sum_{j=1}^N \gamma_j A_j \right) \Phi^n \Big|_{corrected} - \hat{\sigma}^s (\sigma_0, \varepsilon_0, \xi_s, \xi) \end{aligned} \tag{49}$$

Also it should be noted that before calculating the corrected displacement based on the Eq. (49), the \mathcal{X}_j^{n+1} must be modified according to Eq. (50):

$$\mathcal{X}_j^{n+1} \Big|_{corrected} = e^{\left(\frac{-\Delta t}{\tau_j} \right)} \mathcal{X}_j^n \Big|_{corrected} + \gamma_j \frac{1-e^{\left(\frac{-\Delta t}{\tau_j} \right)}}{\frac{\Delta t}{\tau_j}} (\sigma_0^{n+1} \Big|_{corrected} - \sigma_0^n \Big|_{corrected}) \tag{50}$$

By using the above equations, finally the corrected displacement vector is obtained. The velocity and acceleration vectors is corrected base on the corrected displacement vector that obtained from Eq. (50):

$$\dot{\Phi}_{n+1} \Big|_{Corrected} = a_1 (\Phi_{n+1} \Big|_{Corrected} - \Phi_n) - a_2 \dot{\Phi}_n - a_3 \ddot{\Phi}_n \tag{51}$$

$$\ddot{\Phi}_{n+1} \Big|_{Corrected} = \dot{\Phi}_n + a_4 \ddot{\Phi}_n + a_5 \ddot{\Phi}_{n+1} \Big|_{Corrected} \tag{52}$$

It should be noted that Φ_n , $\dot{\Phi}_n$ and $\ddot{\Phi}_n$ were corrected at the end of previous time step (n^{th} time step). So in fact, all parameters of the Eq. (51) and (52) are modified using 3D theory of elasticity. In previous researches that have attempted to correct shear stresses using 3D theory of elasticity, only the transverse shear stress have been modified without correcting the displacement, velocity, and acceleration fields of the plate [23, 83, 87, 88]. While in

this article, in addition to stress, the inertia effects have not been considered too.

2.6. The Proposed Solution Algorithm

There are many numerical methods for solving the obtained constructive equation, among them, Newmark's method is one of the most useful methods for structural dynamic problems [89]. The time-dependent governing system of Eq. (50) is a nonlinear one as well. Due to the nature of the shape memory alloy and dependency of many parameters on ξ of the SMA wires, nonlinearity of the governing equations is of a very complex. Therefore, an iterative method must be used in order to solve this problem. The iterative method starts with an initial guess for required parameters such as displacement vector. The problem is then solved and the displacement is recalculated after updating $\sigma_0, \varepsilon_0, \xi_{s,0}, \xi$ quantities and checking whether a global/local loading/unloading or reverse loading event of SMA wires is in progress, based on the obtained displacement and stress fields. This process is repeated till a proper convergence criterion holds, e.g.

$$\left\| \frac{\Phi_{m+1}^{(r)} - \Phi_{m+1}^{(r-1)}}{\Phi_{m+1}^{(r)}} \right\| < \epsilon \quad (53)$$

Where m and r denote the time step the iteration counter, respectively, and ϵ is a sufficiently small number called the convergence tolerance. The proposed flowchart in Figure 2 shows the main steps of the presented algorithm for solving this complex nonlinear problem. Presented flowchart only summarizes the general steps of the solution. For example, the step to determine the martensitic volume fraction (ξ) and the other properties of SMA itself has a proposed complex algorithm with several steps in which Brinson's constitutive model has been modified, in order to add the cyclical loading and local loading/unloading capabilities and consider the different behaviours of SMA wires in tension and compression that is more realistic assumption. Changes and behaviour of memory alloys everywhere are examined independently. Also, Changes in the properties of the SMA wires at each point of the sandwich panel have been considered independently and continuously over time with the change behaviour of the viscoelastic core by using the proposed algorithm. In such a way that part of the sandwich panel and then the SMA wires can be loaded, while another point of the SMA wires can be in unloaded locally. For example, the time of updating the initial properties of SMA wires such as $\sigma, \varepsilon_0, \xi_{s,0}, \xi$ during cyclic loading/ unloading is determined by presented algorithm. Choosing an appropriate Δt at the beginning of the algorithm is essential for the convergence of the problem and its rate ($\Delta t < \Delta t_{critical}$). However, the algorithm is designed to correct this issue by using bisection technique. The numerical reason for the better convergence in a dynamic analysis when Δt is reduced lies in the role of the mass matrix in the equivalent stiffness matrix.

3. Numerical Results

3.1. Verification of the Results

The results of the modified Brinson's constitutive model and the written code for it are examined at first. For this purpose, the obtained results are compared with the results of the experimental test in the valid reference [90]. The available experimental results are two tensile tests at temperatures of 50 C and -10° C, as shown in Figure 3. The first test was performed at a temperature the end of the above T_{Af} , while the second test was done at a temperature below the T_{Mf} . As can be seen in both tests, the stress-strain curves predicted by the present model are very consistent with the experimental results for two different ambient temperatures. Also, in order to further validate, the natural frequencies and loss factors of sandwich plates have been compared with the results available in valid references [91-93]. The results for the sandwich plate are considered in different modes of boundary condition of all edges clamped (CCCC) and opposite sides clamped (CFCF). The first three natural frequencies, and the corresponding loss factors, are calculated under different boundary conditions of CCCC and CFCF, and are compared with the numerical results obtained by Araujo et al [91] and Huang et al. [92] and experimental result of Wang et al. [93]. All mentioned results are shown in Table 1. As can be seen, results obtained from the presented code and proposed algorithm in different boundary conditions are found to be in good agreement with the published ones.

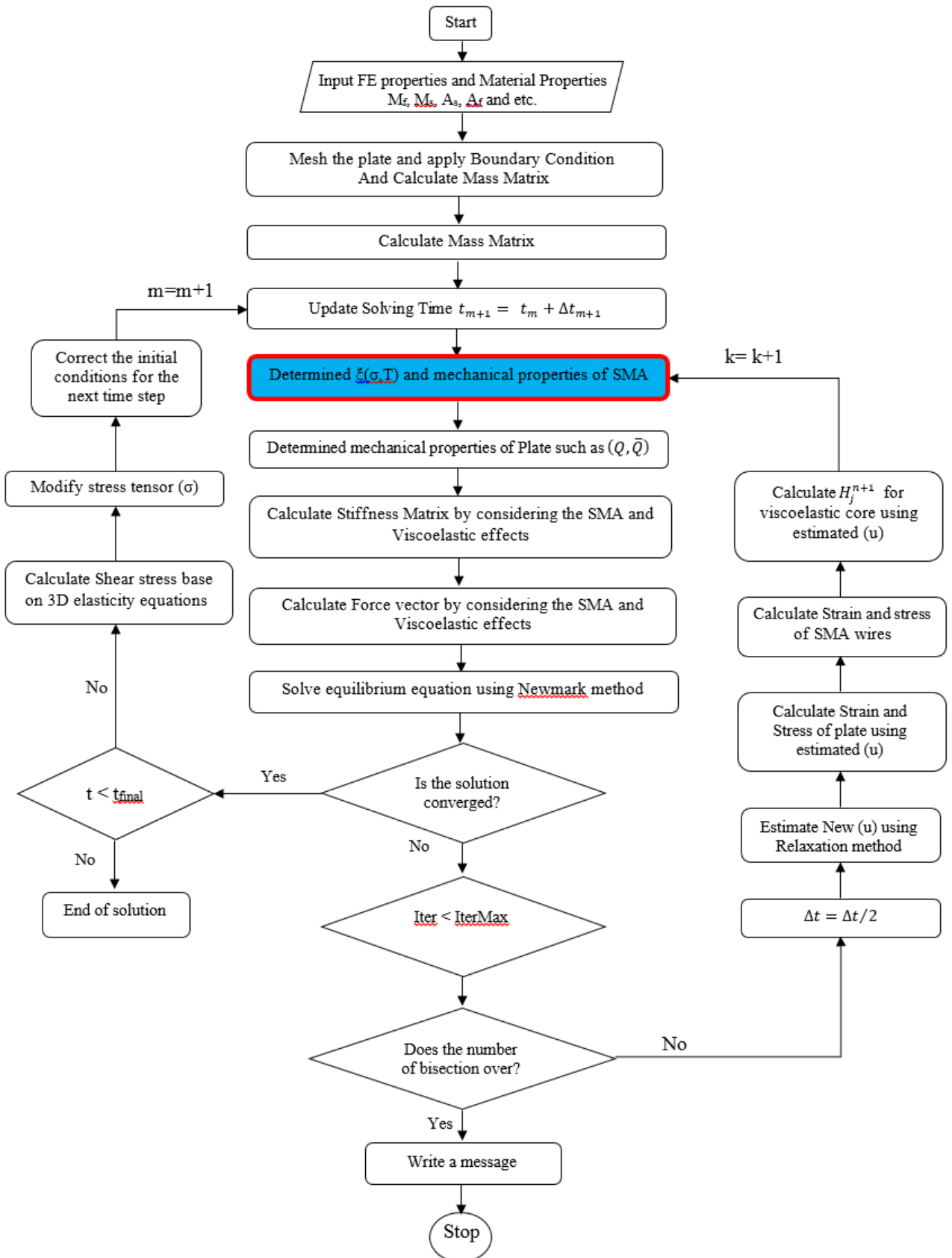


Fig 2: Presented algorithm for solving the dynamic behavior of sandwich panel with embedded SMA wires in composite face sheets and viscoelastic material as a core.

Table 1: Natural frequencies and corresponding loss factors of sandwich plate with viscoelastic core under different boundary conditions.

Mode no.	1		2		3	
	frequenc y	Loss factor	frequenc y	Loss factor	frequenc y	Loss factor
CCCC (Araujo et al., [91])	87.66	0.1886	150.1	0.163	170.99	0.152
Present	87.055	0.1735	145.386	0.1428	177.812	0.153
CFCF (Huang et al., [92])	95.09	0.1315	112.7	0.1274	187.25	0.139
Present	98.0165	0.1861	113.7835	0.1302	184.458	0.120
CCCC (Experimental) (Wang et al., [93])	38	0.092	68.5	-----	90.3	0.158
Present	38.325	0.073	66.128	0.055	87.427	0.125

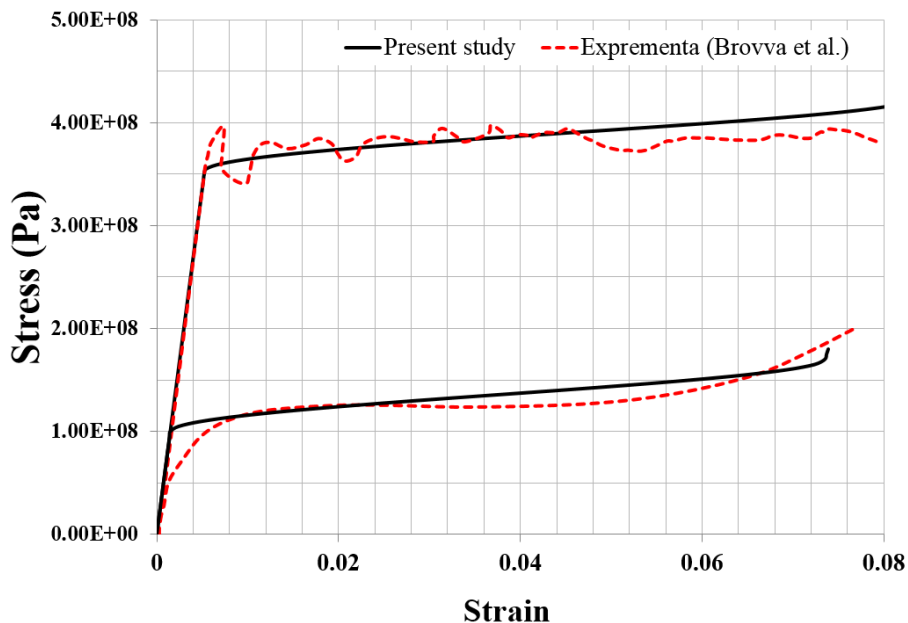


Fig3: Comparing the stress–strain curves predicted by the present model for a monotonically loaded SMA wire with the experimental results [90], in two different ambient temperatures.

4. Sandwich Panel with Viscoelastic Core and Embedded SMA Wires in Composite Face Sheets

In this section the effect of the simultaneous existence of two damping mechanisms of viscoelastic core and embedded SMA wire on the energy absorbing of the structure and on each other has been investigated. For this purpose, three following sandwich panels with exactly the same properties have been analyzed under dynamic loading and the results have been compared:

1. Sandwich panel with viscoelastic core,
2. Sandwich panel with embedded SMA wires in composite face sheets,
3. Sandwich panel including both mentioned damping mechanism.

The plate is loaded by a uniformly distributed rectangular impulse pressure on its upper surface. Effects of the SMA wires and viscoelastic core are studied on the transient responses, i.e. after removal of the applied load. The following non dimensional quantity is defined to extract the results:

$$W = w \frac{100E_2^{skin} h^3}{a^4 q_0}$$

The anisotropic material properties of the embedded shape memory alloy wires and viscoelastic core is presented in Table 2 and Table 3. Mechanical properties of the composite face sheet are as following:

$$E_1 = E_3 = 20.7 \text{ GPa}, E_2 = 221.0 \text{ GPa}, G_{12} = G_{23} = 5.79 \text{ GPa}, G_{13} = 3.29 \text{ GPa}, \nu_{12} = \nu_{23} = 0.23.$$

Table 2.: Properties of SMA material with asymmetric behavior in tension and compression.

$E_A = 33000MPa$	$M_f = 5^\circ C$	$\sigma_f^{cr,-} = 110.6MPa$
$E_M = 18300MPa$	$M_s = 10^\circ C$	$C_M^+ = 6 MPa/^\circ C$
$A_s = 28^\circ C$	$A_f = 32^\circ C$	$\varepsilon_L^- = 0.06$
$\nu = 0.33$	$\rho = 6500 kg/m^3$	$C_A^- = 11.2MPa/^\circ C$
$C_A^+ = 8 MPa/^\circ C$	$\sigma_s^{cr,+} = 40 MPa$	$\sigma_f^{cr,+} = 80 MPa$
$\sigma_s^{cr,-} = 51.8MPa$	$C_M^- = 8.4MPa/^\circ C$	$\varepsilon_L^+ = 0.08$

Table 3: Viscoelastic core material properties [94].

Young's modulus	100 Mpa
Poisson's ratio	0.3
Delayed stiffness (E_∞/E_{eq})	0.2
Relaxation time ($\tau = (\eta/E_\infty)$)	1e-4

Figure 4 shows the dimensionless deformation of the three mentioned cases for the thick and thin sandwich panel. As can be seen, in both the thin and thick sandwich panel, effect of the existence of the viscoelastic core is clearly visible. The best performance in terms of energy absorption, respectively, belongs to the following:

1. Sandwich panel with the viscoelastic core,
2. Sandwich panel with the viscoelastic core and embedded SMA wires,
3. Sandwich panel with the embedded SMA wires.

This is true for both thick and thin panels. Because viscoelastic damping, unlike SMA wires, is not dependent on stress levels, the damping of the viscoelastic core begins with the first cycle and continues until complete energy absorption.

It is noteworthy that the damping of the sandwich panels with viscoelastic core and SMA wires are less than if the sandwich have only viscoelastic core, in both thin and thick sandwiches. In other words, contrary to popular belief, the addition of SMA wires to the sandwich panels with viscoelastic core, reduces the effect of the viscoelastic core and thus reduces the damping of structure. The reason for this is the increased stiffness of the structure due to the presence of embedded SMA wires in the composite face sheets.

While SMA wires are only effective in absorbing structural energy within a determined range of stresses (in the phase transformation area). For this reason, the embedded wires initially played an active role in the damping of the structure, and over time this role faded to eventually disappear altogether. This is clearly seen in the example of thick sandwich panel.

In such a way that the damping of the structure is practically eliminated from the time of 0.04 seconds and the sandwich is continuing to oscillate with a constant amplitude. At this time, the SMA wires are out of phase transformation area due to the stress level and no longer have damping effect in the structure. It should be mentioned that in thin sandwich panel, the embedded SMA wires have not had any effect on the damping of the structure from the very beginning.

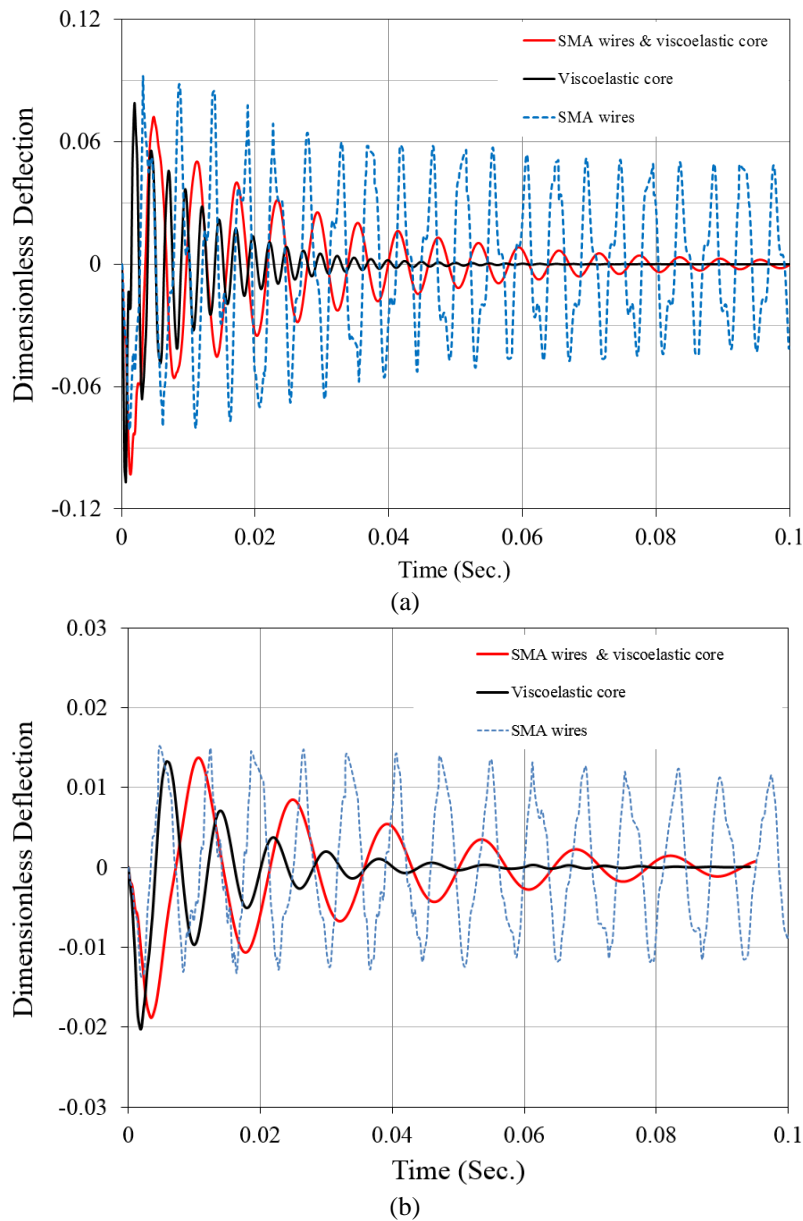


Fig 4: Effect of different damping mechanisms on the time variations of the non-dimensional lateral deflection at the midpoint for: **a)** thick sandwich plate ($a/h = 4$), **b)** thin sandwich plate ($a/h = 10$).

Figure 5 shows the hysteresis loops of the embedded SMA wires in upper and lower layer of the thick sandwich plates with SMA wires and viscoelastic core and the sandwich plates with SMA wires and normal core. As can be seen, in the first cycle, the behavior of both plates (with and without viscoelastic core) in the top and bottom layers is the same. Therefore, the size of the biggest cycles in both plates is equal. But under the influence of the viscoelastic core, the embedded SMA wire loops in the sandwich plates shrink rapidly and disappear after a few cycles. While on the plate with the elastic core, the SMA wires are still active, and are damping the applied energy. Therefore, it can be concluded that the simultaneous existence of two damping mechanisms, viscoelastic core and SMA wires, reduces the effectiveness of each of these mechanisms alone. However, using both mechanism simultaneously increases the damping of the structure. There is also a difference between the behavior of the embedded SMA wires in the upper and lower layers, which is due to the thickness of the plate and the flexibility of the core. The asymmetry behavior of SMA wires in tension and compression is also well evident due to the precise simulation of SMA model.

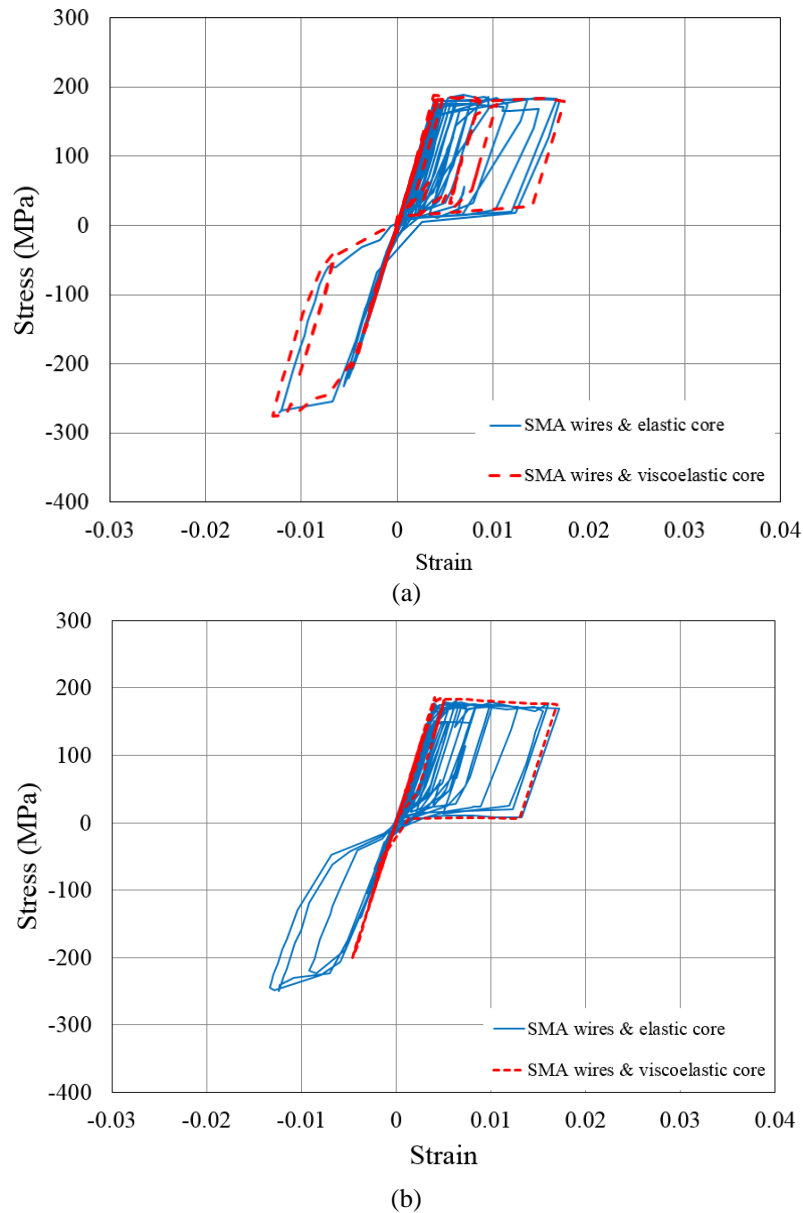


Fig 5: Transformation histories of the embedded SMA wires at the midpoint of the thick sandwich plate ($a/h = 4$) with a viscoelastic core and elastic core: (a) upper layers, (b) lower layers.

Time variations of the martensite volume fraction (ξ) of the midpoints of the upper and lower layers of the thick sandwich plate for both cases are shown in Figure 6. In this figure, the effect of using viscoelastic core on reducing the efficiency of embedded SMA wires can be clearly seen. In a way, the viscoelastic core makes the martensite volume fraction of the SMA wires zero after 0.015 seconds, indicating that the SMA wires are out of phase transformation area. And they no longer have a role in damping the structure. However, structural fluctuations continue to decrease due to the presence of viscoelastic core to eventually be eliminated.

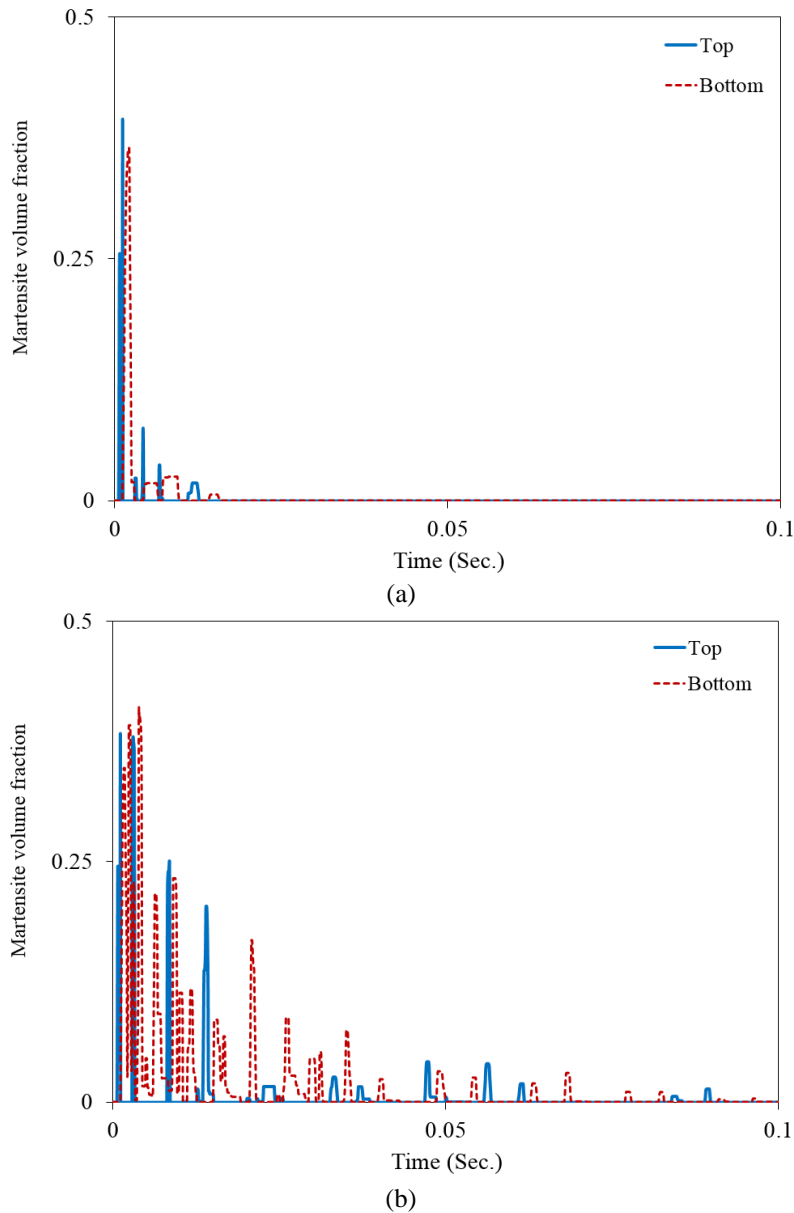


Fig 6: Time variations of the martensite volume fraction of the midpoints of the upper and lower layers of the thick sandwich plate:
 (a) with embedded SMA wires and viscoelastic core, (b) with embedded SMA wires and elastic core.

Transformation histories of the embedded SMA wires of the thin sandwich plates with viscoelastic and elastic core is shown in Figure 7. Totally, in thin plates, the embedded SMA wires have undergone a phase transformation area less than in the thick sandwich plates. This is due to the lower stress level of the embedded wires in the face sheets. For this reason, Figure 4-b shows that the SMA wires did not actually cause a noticeable damping in the structure. As mentioned above, since in these plates the level of the SMA wire's stress is low compared to the required phase transformation stress, adding the viscoelastic core eliminates all the damping effect of the SMA wires. So that the wires in the top layer have only one cycle in the tensile part.

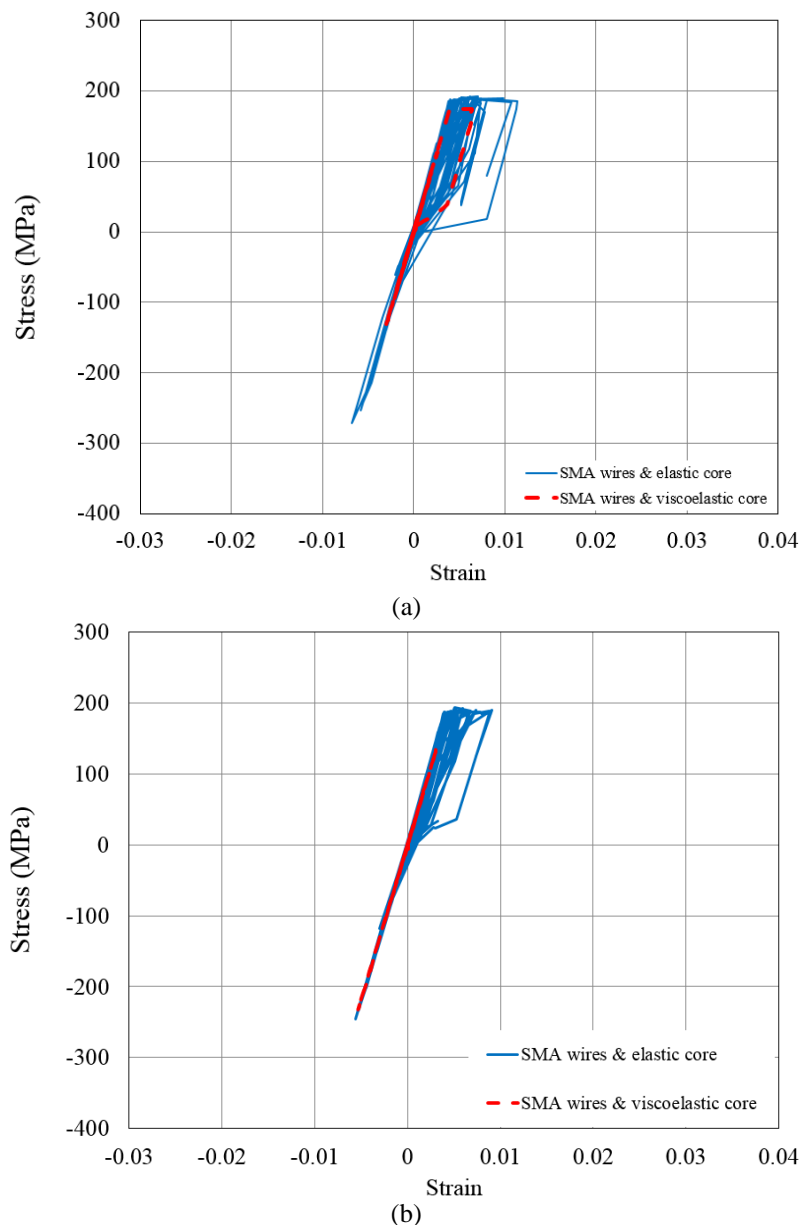


Fig 7: Transformation histories of the embedded SMA wires at the midpoint of the thin sandwich plate ($a/h = 10$) with a viscoelastic core and elastic core: (a) upper and (b) lower layers.

Figure 8 also shows the performance of the embedded SMA wires in a different way. Time variations of the martensite volume fraction of the midpoints of the upper and lower layers of the thin sandwich plate is shown in this figure. This parameter is a component to indicate the phase transformation of the SMA wires. In the case of thin sandwich panel with the embedded SMA wires and viscoelastic core, the SMA wires have virtually no phase transformation and have entered the phase transformation zone in only one cycle, to a very small extent. This can be seen in a different way in Figure 7. While the core is elastic, the SMA wires are relatively more active, although they still enter in to the phase transformation area very little. In general, the effect of embedded SMA wires on thick sandwich panels is greater than on thin panels. This issue is shown clearly in Figure 4 to 8.

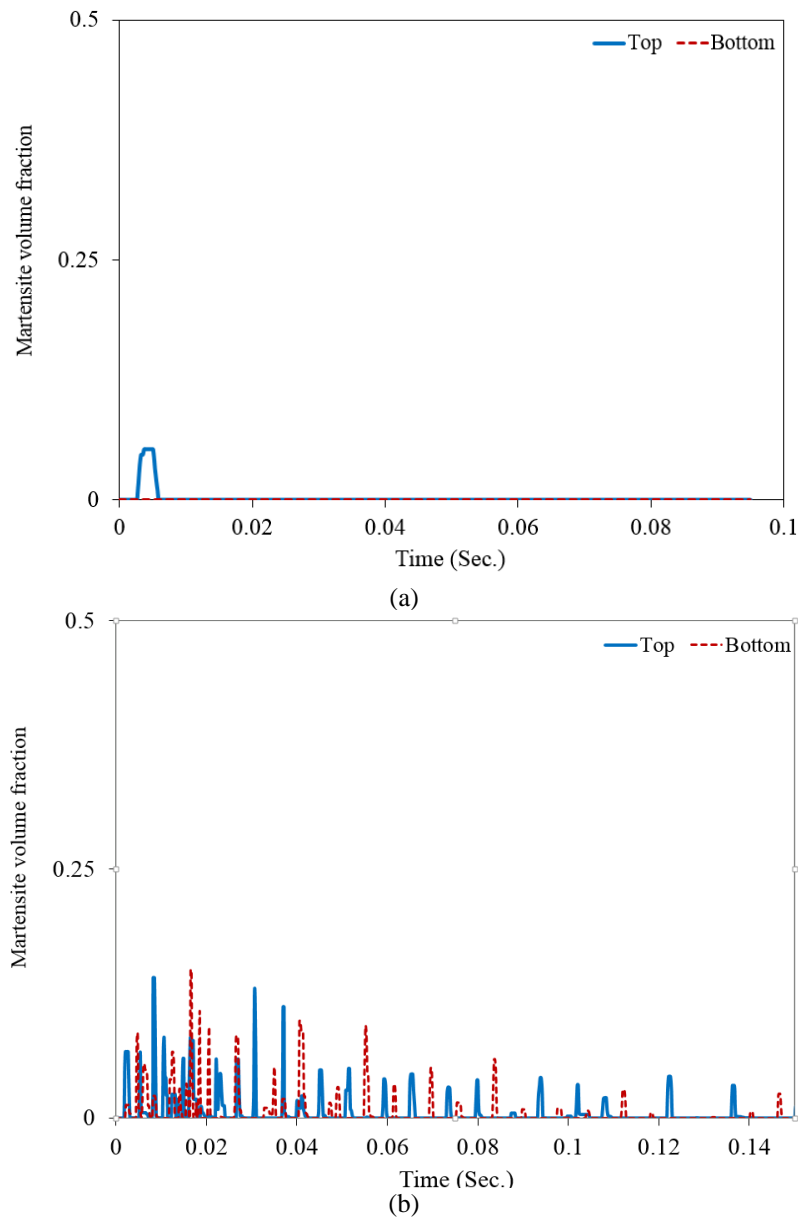


Fig 8: Time variations of the martensite volume fraction of the midpoints of the upper and lower layers of the thin sandwich plate:
(a) with embedded SMA wires and viscoelastic core,
(b) with embedded SMA wires and elastic core.

5. Conclusion

In this paper, the nonlinear dynamic analysis of sandwich plates with the embedded SMA wires in the composite face sheets and viscoelastic core is investigated parametrically. In order to accurately examine the effect of the embedded SMA wires in the composite face sheets, the instantaneous changes in martensitic volume fraction of SMA wires are continuously studied. Also considering the asymmetrical behavior of shape memory alloys in tension and compression are other features of this research. In other words, to analyze the behavior of shape memory alloy wires the kinematic equations of phase transformation of the SMA coupled with the motion equations, which leads to nonlinear and more complex equations. Modified Brinson's constitutive model has been used to model the behavior of SMA wires. In order to consider the effect of viscoelastic core, a standard linear model, which is one of the most suitable models for analyzing solid viscoelastic materials, has been used in real time method. Also, the global-local higher order theory with 3d elasticity correction has been used to solve the equations of the sandwich panel so that in addition to using the high solution speed, the results are also very accurate. Another feature of the

presented theory is considering variation of the sandwich thickness, which is necessary for the analysis of thick sandwich panels, especially with flexible cores. Because in many cases, due to the deformation of the soft core, the behavior of the upper face sheet is practically not similar to that of the lower one, which due to the presence of embedded SMA wires in the composite face sheets and their damping properties, this difference in behavior plays a significant role in dynamic response of the structure. After studied different cases, finally it could be concluded:

- ✓ The effect of embedded shape memory wires on damping is negligible compared to viscoelastic core. However, SMA wires embedded in the thick sandwich panel are more effective than in the thin sandwich panel.
- ✓ Results confirm, for the first time, that the hysteresis loops of the stress-strain loops of the embedded SMA wires may shrink or even disappear in presence of the structural damping such as viscoelastic core; so that, the common belief that two types of damping, i.e., the damping due to the phase transformation and the structural damping are combined without significant interactions, is incorrect.
- ✓ The damping effect of the viscoelastic core, regardless of the stress level of the structure and the applied load to the sandwich panel, starts from the beginning of loading and continues until the moment of complete absorption of the sandwich panel energy.
- ✓ Embedded SMA wires require a certain level of stress to act as a damping mechanism. And this effect gradually decreases until they are completely eliminated and are no longer effective in damping the sandwich panel.
- ✓ In cases where the load applied to the structure is high, the use of Shape memory alloy wires is more effective in the damping of the panel, while if the intensity of the transient load applied to the structure is low, it is better than viscoelastic core to absorb fluctuations and to damp the applied energy.

References

- [1] M. Fremond, *Shape memory alloy*, in: *Shape memory alloys*, Eds., pp. 1-68: Springer, 1996.
- [2] R. S. Lakes, 2017, *Viscoelastic solids*, CRC press,
- [3] D. C. Lagoudas, 2008, *Shape memory alloys: modeling and engineering applications*, Springer,
- [4] W. Ostachowicz, M. Krawczuk, A. Żak, Natural frequencies of a multilayer composite plate with shape memory alloy wires, *Finite Elements in Analysis and Design*, Vol. 32, No. 2, pp. 71-83, 1999.
- [5] W. Ostachowicz, M. Krawczuk, A. Żak, Dynamics and buckling of a multilayer composite plate with embedded SMA wires, *Composite structures*, Vol. 48, No. 1-3, pp. 163-167, 2000.
- [6] T. L. Turner, A new thermoelastic model for analysis of shape memory alloy hybrid composites, *Journal of Intelligent Material Systems and Structures*, Vol. 11, No. 5, pp. 382-394, 2000.
- [7] X.-Y. Tsai, L.-W. Chen, Dynamic stability of a shape memory alloy wire reinforced composite beam, *Composite structures*, Vol. 56, No. 3, pp. 235-241, 2002.
- [8] J.-H. Roh, J.-H. Kim, Hybrid smart composite plate under low velocity impact, *Composite Structures*, Vol. 56, No. 2, pp. 175-182, 2002.
- [9] J.-H. Roh, J.-H. Kim, Adaptability of hybrid smart composite plate under low velocity impact, *Composites Part B: Engineering*, Vol. 34, No. 2, pp. 117-125, 2003.
- [10] Z. Hashin, Viscoelastic behavior of heterogeneous media, 1965.
- [11] Y. Wang, T. Tsai, Static and dynamic analysis of a viscoelastic plate by the finite element method, *Applied Acoustics*, Vol. 25, No. 2, pp. 77-94, 1988.
- [12] R. S. Lakes, A. Wineman, On Poisson's ratio in linearly viscoelastic solids, *Journal of Elasticity*, Vol. 85, No. 1, pp. 45-63, 2006.
- [13] J. Yang, J. Xiong, L. Ma, B. Wang, G. Zhang, L. Wu, Vibration and damping characteristics of hybrid carbon fiber composite pyramidal truss sandwich panels with viscoelastic layers, *Composite Structures*, Vol. 106, pp. 570-580, 2013.
- [14] B. K. Eshmatov, Nonlinear vibrations and dynamic stability of viscoelastic orthotropic rectangular plates, *Journal of Sound and Vibration*, Vol. 300, No. 3-5, pp. 709-726, 2007.
- [15] R. Alex, L. Schovanec, An anti-plane crack in a nonhomogeneous viscoelastic body, *Engineering fracture mechanics*, Vol. 55, No. 5, pp. 727-735, 1996.
- [16] L. Schovanec, J. R. Walton, The quasi-static propagation of a plane strain crack in a power-law inhomogeneous linearly viscoelastic body, *Acta mechanica*, Vol. 67, No. 1, pp. 61-77, 1987.
- [17] A. Assie, M. Eltahir, F. Mahmoud, Modeling of viscoelastic contact-impact problems, *Applied Mathematical Modelling*, Vol. 34, No. 9, pp. 2336-2352, 2010.

- [18] A. Assie, M. Eltaher, F. Mahmoud, Behavior of a viscoelastic composite plates under transient load, *Journal of mechanical science and technology*, Vol. 25, No. 5, pp. 1129-1140, 2011.
- [19] Y. Zhang, G. Jin, M. Chen, T. Ye, C. Yang, Y. Yin, Free vibration and damping analysis of porous functionally graded sandwich plates with a viscoelastic core, *Composite Structures*, Vol. 244, pp. 112298, 2020.
- [20] S. H. Kordkheili, R. Khorasani, On the geometrically nonlinear analysis of sandwich shells with viscoelastic core: A layerwise dynamic finite element formulation, *Composite Structures*, Vol. 230, pp. 111388, 2019.
- [21] M. Sheng, Z. Guo, Q. Qin, Y. He, Vibration characteristics of a sandwich plate with viscoelastic periodic cores, *Composite Structures*, Vol. 206, pp. 54-69, 2018.
- [22] K. S. Ledi, M. Hamdaoui, G. Robin, E. M. Daya, An identification method for frequency dependent material properties of viscoelastic sandwich structures, *Journal of Sound and Vibration*, Vol. 428, pp. 13-25, 2018.
- [23] M. Shariyat, S. Khalili, I. Rajabi, A global–local theory with stress recovery and a new post-processing technique for stress analysis of asymmetric orthotropic sandwich plates with single/dual cores, *Computer Methods in Applied Mechanics and Engineering*, Vol. 286, pp. 192-215, 2015.
- [24] J. N. Reddy, 2003, *Mechanics of laminated composite plates and shells: theory and analysis*, CRC press,
- [25] J. N. Reddy, 2006, *Theory and analysis of elastic plates and shells*, CRC press,
- [26] E. Carrera, S. Brischetto, P. Nali, 2011, *Plates and shells for smart structures: classical and advanced theories for modeling and analysis*, John Wiley & Sons,
- [27] S. M. R. Khalili, M. B. Dehkordi, E. Carrera, M. Shariyat, Non-linear dynamic analysis of a sandwich beam with pseudoelastic SMA hybrid composite faces based on higher order finite element theory, *Composite Structures*, Vol. 96, pp. 243-255, 2013.
- [28] C. S. Babu, T. Kant, Refined higher order finite element models for thermal buckling of laminated composite and sandwich plates, *Journal of thermal stresses*, Vol. 23, No. 2, pp. 111-130, 2000.
- [29] A. Nayak, S. Moy, R. Shenoi, A higher order finite element theory for buckling and vibration analysis of initially stressed composite sandwich plates, *Journal of Sound and Vibration*, Vol. 286, No. 4-5, pp. 763-780, 2005.
- [30] K. Malekzadeh, M. Khalili, R. Mittal, Local and global damped vibrations of plates with a viscoelastic soft flexible core: an improved high-order approach, *Journal of Sandwich Structures & Materials*, Vol. 7, No. 5, pp. 431-456, 2005.
- [31] M. Kheirikhah, S. Khalili, K. M. Fard, Biaxial buckling analysis of soft-core composite sandwich plates using improved high-order theory, *European Journal of Mechanics-A/Solids*, Vol. 31, No. 1, pp. 54-66, 2012.
- [32] M. Shariyat, Thermal buckling analysis of rectangular composite plates with temperature-dependent properties based on a layerwise theory, *Thin-Walled Structures*, Vol. 45, No. 4, pp. 439-452, 2007.
- [33] M. Di Sciuva, U. Icardi, L. Librescu, Effects of interfacial damage on the global and local static response of cross-ply laminates, *International Journal of Fracture*, Vol. 96, No. 1, pp. 17-35, 1999.
- [34] R. G. Lage, C. M. Soares, C. M. Soares, J. Reddy, Analysis of adaptive plate structures by mixed layerwise finite elements, *Composite Structures*, Vol. 66, No. 1-4, pp. 269-276, 2004.
- [35] D. Robbins Jr, J. Reddy, Modelling of thick composites using a layerwise laminate theory, *International journal for numerical methods in engineering*, Vol. 36, No. 4, pp. 655-677, 1993.
- [36] J. Reddy, E. Barbero, J. Teply, A plate bending element based on a generalized laminate plate theory, *International journal for numerical methods in engineering*, Vol. 28, No. 10, pp. 2275-2292, 1989.
- [37] C. Wanji, W. Zhen, A selective review on recent development of displacement-based laminated plate theories, *Recent patents on mechanical engineering*, Vol. 1, No. 1, pp. 29-44, 2008.
- [38] R. Moreira, J. D. Rodrigues, A layerwise model for thin soft core sandwich plates, *Computers & structures*, Vol. 84, No. 19-20, pp. 1256-1263, 2006.
- [39] D. Elmalich, O. Rabinovitch, A high-order finite element for dynamic analysis of soft-core sandwich plates, *Journal of Sandwich Structures & Materials*, Vol. 14, No. 5, pp. 525-555, 2012.
- [40] O. Rabinovitch, Y. Frostig, High-order behavior of fully bonded and delaminated circular sandwich plates with laminated face sheets and a “soft” core, *International journal of solids and structures*, Vol. 39, No. 11, pp. 3057-3077, 2002.
- [41] M. Četković, D. Vuksanović, Bending, free vibrations and buckling of laminated composite and sandwich plates using a layerwise displacement model, *Composite structures*, Vol. 88, No. 2, pp. 219-227, 2009.
- [42] W. Zhen, C. Wanji, Free vibration of laminated composite and sandwich plates using global–local higher-order theory, *Journal of Sound and Vibration*, Vol. 298, No. 1-2, pp. 333-349, 2006.

- [43] A. Ghaznavi, M. Shariyat, Higher-order global-local theory with novel 3D-equilibrium-based corrections for static, frequency, and dynamic analysis of sandwich plates with flexible auxetic cores, *Mechanics of Advanced Materials and Structures*, Vol. 26, No. 7, pp. 559-578, 2019.
- [44] A. Ghaznavi, Modified Global-local theory for investigating composite and sandwich plates under static transverse loading, *نشریه پژوهشی مهندسی مکانیک ایران*, Vol. 20, No. 1, pp. 132-151, 2018.
- [45] A. Ghaznavi, M. Shariyat, Non-linear layerwise dynamic response analysis of sandwich plates with soft auxetic cores and embedded SMA wires experiencing cyclic loadings, *Composite Structures*, Vol. 171, pp. 185-197, 2017.
- [46] M. Shariyat, A. Ghaznavi, Influence analysis of phase transformation anisotropy of shape memory alloy wires embedded in sandwich plates with flexible cores by a third-order zigzag theory with dynamic three-dimensional elasticity corrections, *Journal of Sandwich Structures & Materials*, Vol. 22, No. 5, pp. 1450-1495, 2020.
- [47] M. Mohammadi, A. Rastgoo, Primary and secondary resonance analysis of FG/lipid nanoplate with considering porosity distribution based on a nonlinear elastic medium, *Mechanics of Advanced Materials and Structures*, Vol. 27, No. 20, pp. 1709-1730, 2020.
- [48] M. Mohammadi, M. Hosseini, M. Shishesaz, A. Hadi, A. Rastgoo, Primary and secondary resonance analysis of porous functionally graded nanobeam resting on a nonlinear foundation subjected to mechanical and electrical loads, *European Journal of Mechanics-A/Solids*, Vol. 77, pp. 103793, 2019.
- [49] M. Mohammadi, A. Rastgoo, Nonlinear vibration analysis of the viscoelastic composite nanoplate with three directionally imperfect porous FG core, *Structural Engineering and Mechanics, An Int'l Journal*, Vol. 69, No. 2, pp. 131-143, 2019.
- [50] A. Farajpour, A. Rastgoo, M. Mohammadi, Vibration, buckling and smart control of microtubules using piezoelectric nanoshells under electric voltage in thermal environment, *Physica B: Condensed Matter*, Vol. 509, pp. 100-114, 2017.
- [51] M. Baghani, M. Mohammadi, A. Farajpour, Dynamic and stability analysis of the rotating nanobeam in a nonuniform magnetic field considering the surface energy, *International Journal of Applied Mechanics*, Vol. 8, No. 04, pp. 1650048, 2016.
- [52] A. Farajpour, M. H. Yazdi, A. Rastgoo, M. Loghmani, M. Mohammadi, Nonlocal nonlinear plate model for large amplitude vibration of magneto-electro-elastic nanoplates, *Composite Structures*, Vol. 140, pp. 323-336, 2016.
- [53] A. Farajpour, M. Yazdi, A. Rastgoo, M. Mohammadi, A higher-order nonlocal strain gradient plate model for buckling of orthotropic nanoplates in thermal environment, *Acta Mechanica*, Vol. 227, No. 7, pp. 1849-1867, 2016.
- [54] M. R. Farajpour, A. Rastgoo, A. Farajpour, M. Mohammadi, Vibration of piezoelectric nanofilm-based electromechanical sensors via higher-order non-local strain gradient theory, *Micro & Nano Letters*, Vol. 11, No. 6, pp. 302-307, 2016.
- [55] M. Mohammadi, M. Safarabadi, A. Rastgoo, A. Farajpour, Hygro-mechanical vibration analysis of a rotating viscoelastic nanobeam embedded in a visco-Pasternak elastic medium and in a nonlinear thermal environment, *Acta Mechanica*, Vol. 227, No. 8, pp. 2207-2232, 2016.
- [56] H. Asemi, S. Asemi, A. Farajpour, M. Mohammadi, Nanoscale mass detection based on vibrating piezoelectric ultrathin films under thermo-electro-mechanical loads, *Physica E: Low-dimensional Systems and Nanostructures*, Vol. 68, pp. 112-122, 2015.
- [57] M. Safarabadi, M. Mohammadi, A. Farajpour, M. Goodarzi, Effect of surface energy on the vibration analysis of rotating nanobeam, 2015.
- [58] S. Asemi, A. Farajpour, H. Asemi, M. Mohammadi, Influence of initial stress on the vibration of double-piezoelectric-nanoplate systems with various boundary conditions using DQM, *Physica E: Low-dimensional Systems and Nanostructures*, Vol. 63, pp. 169-179, 2014.
- [59] S. Asemi, A. Farajpour, M. Mohammadi, Nonlinear vibration analysis of piezoelectric nanoelectromechanical resonators based on nonlocal elasticity theory, *Composite Structures*, Vol. 116, pp. 703-712, 2014.
- [60] S. R. Asemi, M. Mohammadi, A. Farajpour, A study on the nonlinear stability of orthotropic single-layered graphene sheet based on nonlocal elasticity theory, *Latin American Journal of Solids and Structures*, Vol. 11, No. 9, pp. 1515-1540, 2014.
- [61] A. Farajpour, A. Rastgoo, M. Mohammadi, Surface effects on the mechanical characteristics of microtubule networks in living cells, *Mechanics Research Communications*, Vol. 57, pp. 18-26, 2014.
- [62] M. Goodarzi, M. Mohammadi, A. Farajpour, M. Khooran, Investigation of the effect of pre-stressed on vibration frequency of rectangular nanoplate based on a visco-Pasternak foundation, 2014.

- [63] M. Mohammadi, A. Farajpour, M. Goodarzi, F. Dinari, Thermo-mechanical vibration analysis of annular and circular graphene sheet embedded in an elastic medium, *Latin American Journal of Solids and Structures*, Vol. 11, pp. 659-682, 2014.
- [64] M. Mohammadi, A. Farajpour, M. Goodarzi, Numerical study of the effect of shear in-plane load on the vibration analysis of graphene sheet embedded in an elastic medium, *Computational Materials Science*, Vol. 82, pp. 510-520, 2014.
- [65] M. Mohammadi, A. Farajpour, A. Moradi, M. Ghayour, Shear buckling of orthotropic rectangular graphene sheet embedded in an elastic medium in thermal environment, *Composites Part B: Engineering*, Vol. 56, pp. 629-637, 2014.
- [66] M. Mohammadi, A. Moradi, M. Ghayour, A. Farajpour, Exact solution for thermo-mechanical vibration of orthotropic mono-layer graphene sheet embedded in an elastic medium, *Latin American Journal of Solids and Structures*, Vol. 11, No. 3, pp. 437-458, 2014.
- [67] M. Mohammadi, A. Farajpour, M. Goodarzi, R. Heydarshenas, Levy type solution for nonlocal thermo-mechanical vibration of orthotropic mono-layer graphene sheet embedded in an elastic medium, *Journal of Solid Mechanics*, Vol. 5, No. 2, pp. 116-132, 2013.
- [68] M. Mohammadi, A. Farajpour, M. Goodarzi, H. Mohammadi, Temperature Effect on Vibration Analysis of Annular Graphene Sheet Embedded on Visco-Pasternak Foundati, *Journal of Solid Mechanics*, Vol. 5, No. 3, pp. 305-323, 2013.
- [69] M. Mohammadi, M. Ghayour, A. Farajpour, Free transverse vibration analysis of circular and annular graphene sheets with various boundary conditions using the nonlocal continuum plate model, *Composites Part B: Engineering*, Vol. 45, No. 1, pp. 32-42, 2013.
- [70] M. Mohammadi, M. Goodarzi, M. Ghayour, A. Farajpour, Influence of in-plane pre-load on the vibration frequency of circular graphene sheet via nonlocal continuum theory, *Composites Part B: Engineering*, Vol. 51, pp. 121-129, 2013.
- [71] M. Danesh, A. Farajpour, M. Mohammadi, Axial vibration analysis of a tapered nanorod based on nonlocal elasticity theory and differential quadrature method, *Mechanics Research Communications*, Vol. 39, No. 1, pp. 23-27, 2012.
- [72] A. Farajpour, A. Shahidi, M. Mohammadi, M. Mahzoon, Buckling of orthotropic micro/nanoscale plates under linearly varying in-plane load via nonlocal continuum mechanics, *Composite Structures*, Vol. 94, No. 5, pp. 1605-1615, 2012.
- [73] M. Mohammadi, M. Goodarzi, M. Ghayour, S. Alivand, Small scale effect on the vibration of orthotropic plates embedded in an elastic medium and under biaxial in-plane pre-load via nonlocal elasticity theory, 2012.
- [74] A. Farajpour, M. Danesh, M. Mohammadi, Buckling analysis of variable thickness nanoplates using nonlocal continuum mechanics, *Physica E: Low-dimensional Systems and Nanostructures*, Vol. 44, No. 3, pp. 719-727, 2011.
- [75] A. Farajpour, M. Mohammadi, A. Shahidi, M. Mahzoon, Axisymmetric buckling of the circular graphene sheets with the nonlocal continuum plate model, *Physica E: Low-dimensional Systems and Nanostructures*, Vol. 43, No. 10, pp. 1820-1825, 2011.
- [76] N. Ghayour, A. Sedaghat, M. Mohammadi, Wave propagation approach to fluid filled submerged visco-elastic finite cylindrical shells, 2011.
- [77] H. Moosavi, M. Mohammadi, A. Farajpour, S. Shahidi, Vibration analysis of nanorings using nonlocal continuum mechanics and shear deformable ring theory, *Physica E: Low-dimensional Systems and Nanostructures*, Vol. 44, No. 1, pp. 135-140, 2011.
- [78] M. Mohammadi, M. Ghayour, A. Farajpour, Analysis of free vibration sector plate based on elastic medium by using new version of differential quadrature method, *Journal of Simulation and Analysis of Novel Technologies in Mechanical Engineering*, Vol. 3, No. 2, pp. 47-56, 2010.
- [79] M. Goodarzi, M. Mohammadi, M. Khoran, F. Saadi, Thermo-mechanical vibration analysis of FG circular and annular nanoplate based on the visco-pasternak foundation, *Journal of Solid Mechanics*, Vol. 8, No. 4, pp. 788-805, 2016.
- [80] M. Sedef, E. Samur, C. Basdogan, Real-time finite-element simulation of linear viscoelastic tissue behavior based on experimental data, *IEEE Computer Graphics and Applications*, Vol. 26, No. 6, pp. 58-68, 2006.
- [81] E. Daya, M. Potier-Ferry, A numerical method for nonlinear eigenvalue problems application to vibrations of viscoelastic structures, *Computers & Structures*, Vol. 79, No. 5, pp. 533-541, 2001.
- [82] Z. Huang, Z. Qin, F. Chu, A comparative study of finite element modeling techniques for dynamic analysis of elastic-viscoelastic-elastic sandwich structures, *Journal of Sandwich Structures & Materials*, Vol. 18, No. 5, pp. 531-551, 2016.

- [83] M. Shariyat, M. Alipour, A novel shear correction factor for stress and modal analyses of annular FGM plates with non-uniform inclined tractions and non-uniform elastic foundations, *International Journal of Mechanical Sciences*, Vol. 87, pp. 60-71, 2014.
- [84] M. Cho, K.-O. Kim, M.-H. Kim, Efficient higher-order shell theory for laminated composites, *Composite Structures*, Vol. 34, No. 2, pp. 197-212, 1996.
- [85] W. Zhen, C. Wanji, A global-local higher order theory including interlaminar stress continuity and C0 plate bending element for cross-ply laminated composite plates, *Computational Mechanics*, Vol. 45, No. 5, pp. 387-400, 2010.
- [86] M. Shariyat, An accurate double-superposition global–local theory for vibration and bending analyses of cylindrical composite and sandwich shells subjected to thermo-mechanical loads, *Proceedings of the Institution of Mechanical Engineers, Part C: Journal of Mechanical Engineering Science*, Vol. 225, No. 8, pp. 1816-1832, 2011.
- [87] V. N. Burlayenko, T. Sadowski, *Dynamic analysis of debonded sandwich plates with flexible core–Numerical aspects and simulation*, in: *Shell-like Structures*, Eds., pp. 415-440: Springer, 2011.
- [88] M. Shariyat, M. Alipour, Semi-analytical consistent zigzag-elasticity formulations with implicit layerwise shear correction factors for dynamic stress analysis of sandwich circular plates with FGM layers, *Composites Part B: Engineering*, Vol. 49, pp. 43-64, 2013.
- [89] J. Argyris, D. Scharpf, Finite elements in time and space, *The Aeronautical Journal*, Vol. 73, No. 708, pp. 1041-1044, 1969.
- [90] M. Brocca, L. Brinson, Z. Bažant, Three-dimensional constitutive model for shape memory alloys based on microplane model, *Journal of the Mechanics and Physics of Solids*, Vol. 50, No. 5, pp. 1051-1077, 2002.
- [91] A. Araújo, C. Mota Soares, C. Mota Soares, Finite element model for hybrid active-passive damping analysis of anisotropic laminated sandwich structures, *Journal of Sandwich Structures & Materials*, Vol. 12, No. 4, pp. 397-419, 2010.
- [92] Z. Huang, Z. Qin, F. Chu, Vibration and damping characteristics of sandwich plates with viscoelastic core, *Journal of Vibration and Control*, Vol. 22, No. 7, pp. 1876-1888, 2016.
- [93] G. Wang, S. Veeramani, N. M. Wereley, Analysis of sandwich plates with isotropic face plates and a viscoelastic core, *J. Vib. Acoust.*, Vol. 122, No. 3, pp. 305-312, 2000.
- [94] A. Assie, M. Eltaher, F. Mahmoud, The response of viscoelastic-frictionless bodies under normal impact, *International journal of mechanical sciences*, Vol. 52, No. 3, pp. 446-454, 2010.